Advancements in tissue and organ 3D bioprinting: Current techniques, applications, and future perspectives

Materials & Design 240 (2024) 112853

Contents lists available at ScienceDirect

Materials & Design

journal homepage: www.elsevier.com/locate/matdes

Review

Advancements in tissue and organ 3D bioprinting: Current techniques, applications, and future perspectives

Mojdeh Mirshafiei [a], Hamid Rashedi [a], Fatemeh Yazdian [b,*], Abbas Rahdar [c,*], Francesco Baino [d,*]

[a] Department of Biotechnology, School of Chemical Engineering, College of Engineering, University of Tehran, Tehran, Iran
[b] Department of Life Science Engineering, Faculty of New Science and Technologies, University of Tehran, Tehran, Iran
[c] Department of Physics, School of Basic Sciences, University of Zabol, Zabol, Iran
[d] Institute of Materials Physics and Engineering, Department of Applied Science and Technology, Politecnico di Torino, Torino, Italy

ARTICLE INFO

Keywords:
Additive manufacturing
Bioprinting
Biomaterials
Bioink
Tissue engineering

ABSTRACT

3D bioprinting techniques have emerged as a flexible tool in tissue engineering and regenerative medicine to fabricate or pattern functional 3D bio-structures with precise geometric designs, bridging the divergence between engineered and natural tissue constructs. A significantly increasing development has been achieved in understanding the relationship between the 3D-printing process and the structures, properties, and applications of the objects created. The ongoing advancement of novel biomaterial inks has enabled manufacturing of models and *in vitro* implants capable of achieving some level of success in preclinical trials. Remarkable progress in cell biology and biology-inspired computational design has assisted in achieving the latest milestone with planned tissue- or organ-like constructs having specific levels of functionality. However, biofabricated constructs still have a long way to go before reaching clinics. This review presents a picture of 3D bioprinting in the context of tissue engineering and regenerative medicine, with focus on biomaterials-related and design-centred aspects. Biomedical applications are described in detail in relation to major tissues or organs considered in the human body. Current technical limitations, challenges, future prospects and improvements are critically outlined and discussed.

1. Introduction

Throughout the past decade, continuous development of tissue engineering (TE) and regenerative medicine (RM) has yielded new therapeutic approaches to regenerate and replace functional tissues and organs [1,2]. In the field of TE and RM, a promising effective technology for generating bioartificial tissue and organ-like structures through an automatic layerwise deposition is an additive manufacturing (AM), commonly referred to as 3D printing [3,4]. Through 3D bioprinting, biomaterials, bioactive molecules, and cells are located layer-by-layer with accurate spatial control [5]. Thereby, patient-specific constructs or implants with hierarchical organization and high resolution can be easily fabricated using medical images or computer design to replicate the intricate geometry and irregular shapes of native tissue [6,7]. To achieve a successful 3D bioprinted tissue, factors that affect the functionality and integrity of resulting bioprinted constructions, i.e. design, technology, and material selection, should be considered [8]. Design considerations allow for more efficient creation and amendment of 3D models and product development, as well as can help identify design mistakes in the earlier validation stage. It is thus vital that printed objects closely resemble their original computer-designed counterparts to avoid costly and cumbersome modifications in the next steps [9,10]. These biostructures, which are used as *in vitro* predictory, diagnostic, and exploratory models, have evolved to produce functional products that have flexibility, scalability, reliability, and durability [11–13].

Compared to conventional TE techniques, 3D bioprinting has many advantages. 3D bioprinting improves on these traditional techniques by implementing automated processes, ensuring high precision, and allowing customization for each application [14]. Scaffolds have been used extensively in TE and RM for many years, However, their ability to accurately replicate the body's native extracellular matrix (ECM) is limited. The use of 3D bioprinting in scaffold construction has improved the microstructures of the scaffolds and made their anatomical features more sophisticated and precise [15,16]. Thus, important anatomical features within the tissue replica, such as the size and location of blood vessels and interconnected pores, can be customized. This customization

* Corresponding authors.
E-mail addresses: hrashedi@ut.ac.ir (H. Rashedi), yazdian@ut.ac.ir (F. Yazdian), a.rahdar@uoz.ac.ir (A. Rahdar), francesco.baino@polito.it (F. Baino).

https://doi.org/10.1016/j.matdes.2024.112853
Received 28 October 2023; Received in revised form 14 February 2024; Accepted 17 March 2024
Available online 19 March 2024

enhances perfusion, neovascularization, and cellular communication, while also enabling the creation of larger 3D bioprinted tissues [17].

However, owing to the complexity of natural tissues and organs, a bioprinter must be able to process and print various biomaterials accompanying diverse cell types simultaneously. Therefore, careful selection of suitable biomaterials inks is essential for successful design and application of 3D bioprinting [18]. There is great versatility in using different biomaterials, whether natural or synthetic and cells to replace or regenerate tissues and organs [19,20]. Cells are deposited in a matrix called bioink, which mimics the physicochemical environment of native tissue and supports cell adhesion, proliferation, and differentiation [21]. Hence, developing bioink formulations that meet both physicochemical and biological requirements for 3D bioprinting applications is one of the enduring challenges of bioprinting [22,23]. In a 3D environment, the interactions between biomaterials and cells have a significant impact on cell viability, proliferation,and differentiation. Therefore, it is necessary to take into account various characteristics of biomaterials, including surface chemistry, hydrophilicity, surface charge, reactivity, roughness, and rigidity [24]. Furthermore, to sustain the embedded cells and facilitate cell adhesion and migration in convoluted structures, internal pore size networks and interconnectivity can be tuned to facilitate mass transfer and the diffusion of nutrients [25]. Nevertheless, a deeper understanding of how environmental stimuli and forces affect the viability of embedded cells during bioprinting is required to make bioinks amenable to bioprinting [26]. The properties of bioinks, such as their rheology, photoreactivity, thermal and oxidative stability and their significance should be always related to the specific bioprinting technique used [27]. In other words, different bioink properties are advisable for different 3D bioprinting techniques, which are able to fabricate either acellular or cellular constructs in a precise and controlled way [28]. Based on the progress of ongoing research in this field, the tremendous potential for the fabrication of multifunctional tissue-engineered compounds with unprecedented capability to meet challenges explains its increasing popularity [29,30].

The present review is focused on tissue- and organ-based 3D bioprinting to achieve regenerative alternatives. We briefly summarized and evaluated various currently applied bioprinting techniques. This is followed by an overview of potential TE and RM applications regarding 3D bioprinting. This application is then described in detail in relation to various organ systems of the human body. Tissues and organ bioprinting of major organ systems, including skin, bone, cartilage, skeletal muscle, tendon, dental, cornea, cardiovascular, neural, liver, glands, respiratory system, urinary system, and reproductive system are reviewed. Ultimately, we pointed out the current main challenges and future perspectives related to manufacturing 3D bioprinting *in vitro* models. The development of future approaches based on this understanding can facilitate the fabrication of functional organs and pave the avenue to development of fully bioprinted organs.

2. Overview of 3D bioprinting techniques

2.1. Fundamentals

The process of bioprinting involves fabricating functional tissues and organs by integrating and assembling various biomaterials and bioactive molecules in 3D. Bioprinting techniques provide reasonable control over both acellular constructs and cell-laden constructs according to mimicking a specified configuration as well as surface and structural properties leading to steering cell activity [31]. The workflow of bioprinting techniques commonly starts from medical image datasets such as magnetic resonance imaging or computed tomography (CT) [32] which provide macrostructure information of organs and tissues; then, the architecture of 3D structures with high fidelity is achieved through computer-aided design (CAD) software [33,34](Fig. 1). Successful use of

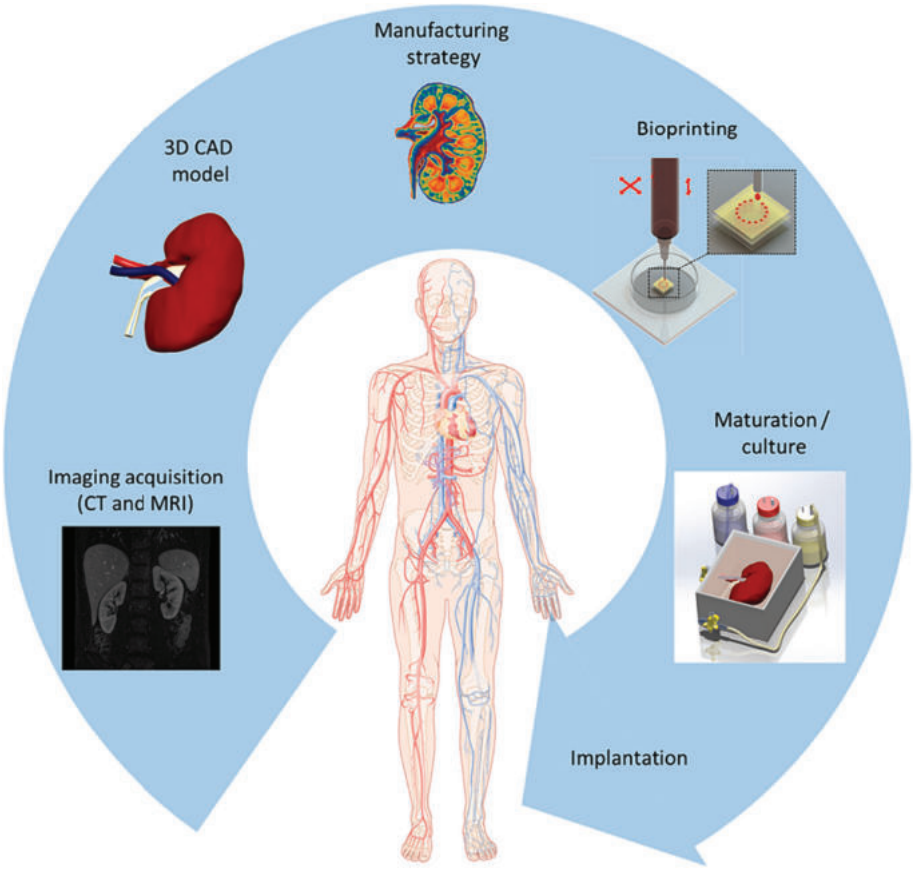

Fig. 1. Schematic illustration of the steps required to generate bioprinted tissue structures. Reproduced with permission from Ref. [31] Copyright 2020 ACS.

bioprinting technology is attributed to the functionality of the resulting structure, which is defined based on the components, bioprinting device, and cell–cell interactions [35]. Several techniques have been developed to allow accurate and controlled deposition different biomaterials, resulting in the creation of intricate structures that mimic native tissues and organs [5]. In this overview, we will explore three commonly used 3D bioprinting techniques, based on the principle of operation which are classified as Inkjet-based, laser-based, and extrusion-based bioprinting.

Inkjet-based bioprinting operates on the same principles as traditional inkjet printing, but instead of ink, it uses bioink-containing living cells. This technique involves the precise ejecting droplets of bioink from a print head onto a substrate to form a specific 3D structure [36]. Inkjet-based bioprinting is considered a non-contact technique which creates discrete droplets under pressure and precisely deposits them onto a substrate at desired locations under computer control where interactions between the droplets and substrate are created [37]. Pressure pulses impact the fluid chamber by overcoming the surface tension of bioink, triggering droplet ejection, according to various actuator mechanisms (thermal, piezoelectric, electrostatic, etc.), causing droplet ejection. To eject droplets of various sizes during the printing process, inkjet printheads are temporarily deformed either thermally or piezoelectrically. The thermal inkjet printer uses a heating pulse from a thermal actuator to eject the vapor bubble and ink droplets from the nozzle [38]. The piezoelectric inkjet bioprinting technique, on the other hand, relies on piezoelectric actuators that generate transient voltage pulses that induce deformation of the bioink chamber, thereby overcoming surface tension and ejecting bioink droplets from a nozzle. By adjusting the applied voltage, the droplet size, and shape can be controlled [39]. Droplet size and dispensing rate are affected by ink solution fluid characteristics (such as surface tension and viscosity), nozzle diameter, and frequency at which printing heads deform [39,40]. Inkjet-based bioprinting allows high-speed and high-resolution printing, making it suitable for creating intricate patterns with high cell density. However, it may have limitations in terms of printing viscous bioinks and retaining cellular viability during the printing process [36].

Laser-based bioprinting uses a mechanism similar to inkjet printers, using laser pulses to precisely deposit cells and biomaterials onto substrates. This technique involves creating a laser-induced pressure wave that propels cell-containing droplets from a donor slide to a receiving substrate, forming a desired pattern [41]. A pulsed laser beam is directed onto the interface between the target substrate and the absorbing layer. This causes thermal volatilization and the formation of microbubbles. Bioink droplets are ejected by the expansion of microbubbles. Initial bioprinting systems using laser-based processes were also referred to as stereolithography (SLA). The SLA bioprinting technique utilizes visible light or ultraviolet to layer by layer photopolymerize a photosensitive solution in specific areas to generate suitable structure. Thanks to the laser beam's small size, SLA can produce cell patterns with intricate structures and achieve high submicron printing resolution [42–44]. The digital light processing (DLP) and SLA technique both use photosensitive materials, but their procedure differs. During the DLP process, a digital micromirror device is used to target light onto a region that crosslinks all the points related to each layer [42,45].

Other laser-based techniques techniques have been employed by combining techniques like pressure-based bioprinting with light-emitting diodes (LEDs), which crosslink materials upon extrusion. In contrast to the selective crosslinking of materials, other laser-based bioprinting techniques selectively dispense bioinks, comparable to droplet-on-demand [46]. These laser processes are referred to as laser-induced forward transfer (LIFT). In this process, a glass slide that has been coated with an absorbed layer is focused with a fast-pulse laser beam, vaporizing the layer and resulting in the formation of droplets. The LIFT technique provided precise cell-laden bioprinting on small-size structures and it can be used with a wide variety of bioinks with different properties [31,47]. Another light-based bioprinting technique is two-photon polymerization (2PP), which produces 3D structures by simultaneously absorbing two photons from a femtosecond (fs) near-infrared laser pulse. This technique can achieve high resolution, with 3D structures ranging in size from nanoscale to millimeters [48]. Laser-based bioprinting techniques are non-contact nozzle-free technique that avoids cell shearing and enables high cell density and highly viscous materials to be used for tissue construction [49]. Laser-based bioprinting offers high precision, allowing the printing of single cells, cell aggregates, or biomaterials with subcellular resolution [50]. It enables the creation of intricate tissue structures by spatially controlling the deposition of various cell types. However, equipment complexity, expense, and the need for specialized materials may limit its widespread application [51–53].

Extrusion-based bioprinting is one of the most common and versatile techniques used in 3D bioprinting. It involves the deposition of biomaterial ink continuously through a nozzle using mechanical force or pressure driven by a delivery system such as air, a piston, or a screw. The bioink is carefully extruded layer by layer to print a desired structure [54,55]. The pneumatic extrusion-based bioprinting drive system is simple and primarily dependent on pneumatic pressure, while the mechanical drive mechanism provides better spatial control. Furthermore, mechanical techniques regulate the bioink more directly than pneumatic systems, which rely on the delayed response of compressed gas in pneumatic systems. Nonetheless, pneumatic systems offer some advantages when applying various types and viscosities of bioinks by adjusting valve gate time and pressure. Both pneumatic and mechanical techniques can print highly viscous bioinks, though the mechanical system might offer superior spatial control [56]. The resolution of extrusion-based bioprinting is typically influenced by pressure, nozzle diameter size, deposition rate, and material type, but the achieved printing resolution is relatively low, ranging from 200 to 1000 μm, compared to other bioprinting techniques. This technique offers high resolution and allows for the inclusion of multiple cell types or growth factors in the bioink [58]. Moreover, its ease of use, scalability, as well as wide range of applicable biomaterials make it a preferred technique for printing biomimetic 3D tissue constructs. However, passing bioink through the nozzle diameter may raise shear stress, leading to a decrease in cell viability; this a challenging point needing optimization and affects the printing speed and the size of cell aggregates that can be printed [57]. The most widely used technique for material extrusion in 3D bioprinting is the fused deposition model (FDM) which is a type of extrusion-based technique. Despite having lower surface quality and precision than other 3D bioprinting techniques, FDM is extensively employed in the biomedical field for create 3D scaffolds because of how simple it is to use, how flexible its operating temperatures are, and how inexpensive it is to maintain [58].

2.2. Integration of 3D bioprinting with other approaches

3D printing indeed offers a versatile approach for fabricating customized biomaterial scaffolds with interconnected pore networks that facilitate the transport of proteins, oxygen, and nutrients compared to traditional techniques [59]. However, many existing 3D printing methods lack the resolution required to produce filaments suitable for scaffolds across a range of tissues. Additionally, the pore sizes of 3D-printed scaffolds are often larger than the size of cells, adversely affecting cell seeding efficiency and tissue formation [60]. Micro/nanopatterning has emerged as a significant technique for designing scaffolds that control the morphology and arrangement of cells. Among these techniques, electrospinning stands out as a robust and straightforward method that employs high voltage to generate nanoscale fibers with a large specific surface area. Electrospinning enables the alignment and elongation of polymer chains, resulting in nanofibers with a well-defined structure that mimics the physical functions of the native ECM. These nanofibers provide numerous attachment points for cell adhesion and growth, influencing cell morphology and activities [61]. Moreover, electrospun nanofibers offer a viable platform for the delivery

and controlled release of drugs, peptides, or bioactive factors by immobilizing them on the fiber surface or encapsulating them within the fibers. However, the mechanical performance of electrospun fibers is often limited, and there is a need to fabricate novel products and devices of various shapes to expand the applications of electrospinning in biomedicine [62].

To address these limitations, the combination of 3D printing and electrospinning techniques proves to be advantageous. This integration allows for the creation of materials with controlled shape, highly porous interconnected structure, sufficient support strength, and ability to incorporate nanopatterning. It also provides ECM-like niches and bioactive cues to cells. Depending on the specific application, 3D-printed scaffolds and electrospun fibers can be combined in various ways, such as electrospinning onto 3D-printed scaffolds, 3D printing onto electrospun fibers, alternating the use of 3D printing and electrospinning, using electrospun fibers as inks for 3D printing, decorating/infusing 3D-printed scaffolds with electrospun nanofiber segments, or fabricating electrospun scaffolds on 3D-printed collectors/templates. The incorporation of sacrificial materials in these processes brings new challenges and opportunities into the fiber fabrication process [63].

On the other hand, in order to facilitate the advancement of 3D bioprinting technology from basic tissue creation in laboratories to the development of fully functional and implantable organs, it is necessary to achieve both shape control and functional control. This entails replicating the cellular composition of native tissue at the microscale, enabling interactions between different cell types to achieve the desired function [64].To accomplish this, precise and controllable multi-material printing is essential, potentially even at the resolution of individual cells. The lack of microscale precision during mesoscale fabrication hampers the arrangement of distinct cell types within tissue assemblies. However, it is the microenvironment created by cell-to-cell signaling that influences primary cell differentiation and leads to spontaneous morphogenesis [65,66]. Consequently, the absence of accurate microscale cell placement affects the morphology of macroscale organoids and limits the reproducibility and applicability of artificial tissues [67].

To fabricate artificial biological tissues that function comparably to natural ones, it is critical to position specific cell types in multiscale structures with hierarchical features that mimic the microscale environment of natural tissues. Therefore, a multi-material, bottom-up biofabrication approach would be highly advantageous [68]. Researchers have begun addressing these challenges by combining the cell and fluid manipulation capabilities of microfluidics with the biofabrication potential of 3D bioprinting. Microfluidic biofabrication techniques leverage the cell and biomaterial handling capabilities offered by microfluidic devices to enhance microscale precision [64]. The geometrical constraints imposed by microfluidic devices, where lower-dimensional forces such as viscous forces and surface tension dominate, enable the generation of well-defined patterns by controlling fluids containing biomolecules, cells, organisms, or chemical agents. These constructs can consist of various biomaterials or cell-laden bioinks. Furthermore, the microfluidic environment with multiple inlets allows for the provision of growth factors and nutrients during the printing process, thereby enhancing cell viability and guiding primary cell differentiation. Additionally, the seamless transition between materials becomes feasible within the microfluidic setup [68–70].

3. 3D bioprinting in TE and RM

Regeneration or transplantation is required for severe tissue damage caused by disease or trauma. In TE, the integration of biology and engineering principles can be applied to replace, repair, and regenerate damaged, lost, or diseased tissue and organ through the implantation of scaffolds. This field is rapidly expanding to address the limitations of donor tissue and immune responses [71]. To achieve desirable mechanical properties and mass transport, scaffold design should be flexible enough to create intricate 3D structures with hierarchical porous architectures mimicking native tissues.This will allow mechanical functionality to be coupled with tissues and organs regeneration [72]. However, traditional fabrication techniques such as solvent casting, gas forming, and freeze drying, etc. have limitations when it comes to scaffold designs with complex topologies and sufficient mechanical properties [73]. In TE, bioprinting allows for the fabrication of intricate tissue structures with controlled microarchitecture, allowing for the recreation of biological structures at a cellular level [74]. This technology offers the potential to address the limitations of traditional TE approaches, such as cell seeding onto scaffolds, by allowing cells to be placed directly in a controlled manner. Bioprinting can create intricate tissue structures with high cell viability and precise control over cell distribution, which is crucial for effectively regenerating functional tissues [75].

Bioprinting, on the other hand, plays a significant role in this field by providing a platform to fabricate patient-specific tissue structures. By using a patient's own cells, bioprinting can generate personalized tissue grafts that minimize the risk of immune rejection. This personalized approach has the potential to revolutionize transplantation and facilitate the regeneration of damaged tissues, such as skin, bone, cartilage, and even organs [76,77]. Bioprinting also allows for the incorporation of bioactive substances such as drugs or growth factors into the printed constructs. This enables the controlled release of these factors, enhancing the regeneration process and promoting tissue healing [78]. In addition to fabricating complex tissue architectures with multiple cell types, bioprinting has the advantage of creat vascular networks, and intricate microenvironments which is crucial for the successful regeneration of functional tissues that closely resemble their natural counterparts.

A successful 3D-bioprinted tissue should exhibit several key characteristics. Firstly, it must be capable of replicating tissue-specific vascular networks within a specific size range. Additionally, it should possess mechanical properties that closely match those of the host tissue. Lastly, it should be able to integrate with the body's vascularization system effectively, thereby maintaining tissue functionality [79]. Vascularization is crucial for the viability and utility of the host tissue. Without proper vascularization, the implanted tissue would not be able to survive for an extended period. Vascularization allows the implanted tissue to establish functional connections with the existing tissue *in vivo*. Consequently, the synergy between 3D bioprinting and vascularization strategies is of paramount importance [80]. While progress has been made in developing strategies for vascularization in bioprinted tissue and organ substitutes, the inclusion of fully functional vascular networks remains a significant challenge in the field of TE and RM. The first challenge is to replicate the layered structures of blood vessels biologically, including the specific cells and proteins, to ensure proper functioning. Another critical challenge in 3D bioprinting of vascularized tissues is the precise production of complex hierarchical vascular networks that are anatomically compatible with the host tissues. This requires precise positioning of various biomaterials, endothelial cells (ECs), vascular smooth muscle cells (SMCs), and growth factors to enhance the development of robust vasculature [81]. A commonly used strategy to promote the growth of blood vessels in implanted tissues is to apply pro-angiogenic growth factors, which help attract the host's blood vessels. Making bioinks containing bioactive agents, which can promote angiogenesis and the formation of capillaries, is one promising strategy [79]. Achieving these goals necessitates a comprehensive understanding of embryonic development, mechanobiology, cell–cell, and cell-material interactions, as well as the biological responses of endothelial cells to various stimuli, such as perfusate flow and hydrostatic pressure [81].

The following sub-sections highlight the major applications of 3D bioprinting for TE and RM; an overview is also reported in Table 1.

Table 1
3D bioprinting applications in TE and RM.

Application	Bioink	Cell line	Printing technique	Outcome	Refs.
Skin	Sodium alginate (SA)-gelatin (Gel)	RS1s & HUVECs	Extrusion	- Promotion of diabetic wound healing via antioxidant, anti-inflammatory, proangiogenic effects. - Increase of the level of SOD & removal of excess ROS. - Increase of the level of TGF-β & decrease of the expression of TNF-α, IL-6, and IL-β. - Promotion of cell migration & angiogenesis *in vitro*.	[229]
	GelMA-hyaluronic acid methacryloyl (HAMA)-adECM	ADSCs	Extrusion	-Better wettability, degradability, cytocompatibility. -Promoting angiogenesis and collagen synthesis. -Full-thickness skin defect healing in a nude mouse model.	[230]
	GelMA-chitosan nanoparticles (CSNPs)	nHDF	Extrusion	-Proper antibacterial & cell proliferation activity. -Accelerated wound healing in rats models.	[231]
	GelMA-nano-cellulose (BNC)	HDF & HaCaTs	Extrusion	-High printability & cell-friendly sparse microenvironment. -Remodelling of the ECM & supported epidermis reconstruction. -Promotion of granulation tissue regeneration & improvement of wound healing quality.	[232]
Bone	Chitosan/ Nanohydroxyapatite/ Hydroxyethyl-cellulose	Ad-MSCs & MG-63, & RAW 264.7	Extrusion	-Improvement of cell attachment. -Gradual release of ALN during 50 days. -Inhibition of osteoclast activity & stimulation of stem cells to regenerate the ECM at the vulnerable site.	[233]
	Alginate/β-tricalcium phosphate (β-TCP)	MG-63	Extrusion	-Superior physical properties. -Promotion of cell viability & alkaline phosphatase activity.	[234]
	GelMA/methacryloyl alginate (AlgMA)	ACPCs & BMSCs	Extrusion	-Excellent printability at room temperature & maintainance of high cell viability. -Chondrogenic ability of ACPCs & osteogenic ability of BMSCs. -Inherent differential spatial regulation of ABLHs. -Achievement of harmonious cartilage–bone interface by ABLHs.	[235]
	Methacrylated collagen (CMA)	SCs & BMSCs	DLP	-Higher proliferation rate & expression of neural stem cell-associated genes. ->95 % cellular viability, better cell spreading & higher expression of osteogenesis-related genes.	[236]
Cartilage	Methacrylated hyaluronic acid/gelatin methacryloyl (HG)	C28/I2	Dual-channel	-Promotion of cell migration, proliferation, chondrogenic differentiation, ECM deposition. -Alteration of macrophage polarization & regulation of the expression of inflammatory cytokines.	[237]
	Methacrylated HA (MeHA)-Col I & MeHA-Col I/Col II	MSCs	Extrusion	-Col II inclusion enhanced hydrogel-embedded MSC chondrogenesis	[238]
	Composite nanocellulose (NFC, NCC and NCB)-alginate	hNSCs	Pneumatic	-Superior print resolution of NFC. -Best post-printing shape fidelity of NCB -Increase in chondrogenic gene expression & ECM production. -Increase in cell number & metabolism.	[239]
	GelMA/hydroxyapatite (nHAp) & tyramine-modified hyaluronic acid (THA)	hOBs	Extrusion	-GelMA/nHAp hydrogels maintained the osteogenic properties of osteoblasts in a short time. -THA maintained the chondrogenic properties of chondrocyte micropellets.	[240]
Skeletal muscle	GelMA/collagen/dECM	C2C12 & hASCs	Optic-fiber-assisted	-Higher degrees of cell alignment & myogenic activities. -Induction of greater muscle regeneration than the cell construct without topographical cues. -Improvement of *in vivo* VML repair.	[241]
	GelMA/AuNPs or MXene nanosheet	C2C12	Extrusion	-Enhancement of printability & biological properties. -Increase of conductivity. -Improvement of rheological properties & printability.	[242]

(*continued on next page*)

Table 1 (*continued*)

Application	Bioink	Cell line	Printing technique	Outcome	Refs.
	Fibrinogen/gelatin	C2C12	Pneumatic	-Dynamic changes of skeletal muscle tissue during *in vitro* 3D construction. -The differentiation of myotubes in the thinner 3D bioprinting muscle-like bundles was higher. -The width of the structure and the force generated affect the orientation and maturity of the muscle fibers.	[122]
Cornea	HA with dopamine & carbohydrazide modification (HA-DA-CDH)	hASCs	Extrusion	-Cellular growth & tissue formation alter the mechanical properties of the bioprinted composite constructs significantly. -Good integration of bioprinted composite with host tissue in ex vivo cornea organ culture model.	[243]
	CECM-GelMA	hCFs	DLP	-Favorable properties (high dynamic strength and compression stress, biocompatibility, and *in vivo* recoverability). - Promotion of epithelial regeneration, maintaining the matrix aligned, & restoration of clarity.	[244]
	GelMA	Corneal Stromal	SLA	-Promotion of cell attachment, growth, and integration within the scaffold. -Increase of gene expression of collagen type I, lumican and keratan sulfate.	[245]
Cardiovascular	Nanofibrillar cellulose/alginate gels	HEK293 & HUVECS	Extrusion	-Reproducible manufacturing; similar elongation, ultimate tensile strength, and compliance as a porcine aorta. -Blood pressure-resistant, compliant, stable, and cell culture-compatible structures, & degradation *in vitro* on demand.	[246]
	Alginate-gelatin	iCMs & HCAECs &CF	Extrusion	-Significant improvement in cardiac function by epicardial transplantation in mice modelling MI. -Gene expression changes only for the spheroid treatment group. -Similar gene expression profiles for Sham and mice treated with cardiac spheroid patches.	[247]
	MeTro/GelMA	HUVECs & CFs	Extrusion	-The printed constructs demonstrate endothelium barrier function and spontaneous beating of cardiac muscle cells -Minimal inflammatory responses & efficiently biodegraded *in vivo*.	[248]
	cdECM/Laponite-XLG nanoclay/poly(ethylene glycol)-diacrylate (PEG-DA)	HCFs & hiPSC & HS27A	Extrusion	-Shape fidelity, adaptability to different printing conditions, and high cell viability. -The bioinks support the survival of less robust cardiac cells.	[249]
Neural	GelMA	hiPSC & hNPC & SH-SY5Y	Extrusion	-Support to neural cell survival & modulation of neural differentiation.	[250]
	Poly(ethylene glycol)/Arg-Gly-Asp and Tyr-Ile-Gly-Ser-Arg peptide motifs and full-length collagen IV at a stiffness similar to the human brain	iPSC & BMECs	Drop-on-demand	-Support of endothelial-like vasculogenesis & enhancement of neural differentiation and spontaneous activity.	[251]
	Gel/CNF	NSCs	Coaxial	-Biophysical and biochemical cues. -Improvement of the motor function recovery via mediating the complicated environment at the initial stage after SCI. -Regulation of cell function.	[252]
	Fibrin/PCL–retinoic acid (RA)-purmorphamine (puro)	hiPSC	Microfluidic	-Homogeneously distribution of drug-loaded microspheres within the fibers of the constructs. -Promotion of an efficient differentiation and maturation of MNs. -Expression of the markers associated with GABAergic neurons and astrocytes. -Responsiveness upon stimulation with Ach.	[253]
Liver	Alginate/ cellulose nanocrystal/GelMA	NIH/3T3 & HepG2	Microextrusion	-Excellent shear-thinning behavior. -High printability without cell damage. -Improvement of hepatic cell function.	[254]
	decellularized liver extracellular matrix (dLM)/gelatin/ PEG	HepG2	Extrusion	-Improvement of rheology, extrudability, and mechanical stability. -Support to cell growth & liver-specific functions.	[255]
	dLM-PEG-tyrosinase	HepG2 & NIH 3 T3	Extrusion	-Good cell viability & spreading. -High crosslinking, cytocompatible gelation with	[256]

(*continued on next page*)

Table 1 (*continued*)

Application	Bioink	Cell line	Printing technique	Outcome	Refs.
				superior rheological properties and diffusion. -Increase of albumin secretion & consistent hepatic gene expression *in vitro*.	
Glands	Alginate–gelatin	KCs & Fbs & MSCs	Extrusion	-Overcaming of the difficulties in simultaneously inducing Sweat glands (SG) and hair follicle (HF) regeneration. -Promotion of both SG and HF differentiation. -Promotion of SG and HF genesis.	[257]
	Alginate–gelatin	MSCs	Extrusion	-Direct MSC differentiation. -Regulation of MSC fate decisions. -Facilitation of SGs recovery.	[258]
	Alginate–gelatin	MSCs &	Extrusion	-Notch4 enhances MSC stemness & promote SG differentiation. -Reduction of keratin 19-positive epidermal stem cells & keratin 14-positive SG progenitor cells by inhibiting Notch4 -Delayed embryonic SG morphogenesis *in vivo*.	[259]

3.1. Skin

Human skin is the most extensive body tissue; it has unique and intricate anatomy mainly consisting of multiple layers of cells as well as functional units such as blood vessels, sweat and sebaceous glands. The skin is composed of three layers: the epidermis, dermis, and hypodermis. Different skin cells are located in these layers based on region specificity: melanocytes and keratinocytes are the main components of the epidermis, fibroblasts lie in the dermis and there is adipose tissue at the base of the hypodermis; meanwhile, all layers contain collagen [82,83]. As the first defense barrier, the skin serves various protective functions, including protection against potential environmental hazards such as physical injury, radiation, dehydration, pathogens, toxic chemicals, etc. In addition, the skin has regulatory functions for body temperature, maintains the integrity of the body, and acts as a sensory interface with the environment [84].

Nonetheless, since skin is the body's outermost layer, it is prone to various damages. In slight injuries, the body can naturally produce fibrin and collagen to self-repair the skin, but for severe irreversible wound damage, skin substitutes are required [85]. An ideal skin substitute should mimic the elasticity of natural skin tissue, resist infections, prevent dehydration and not cause reduced sensitivity, scarring, or skin discoloration [86]. 3D bioprinting has potential to address limitations of conventional skin regeneration and replacement methods and meet clinical needs as a promising strategy for the reliable, rapid, and scalable generation of biomimetic skin substitutes [85]. Moreover, bioprinting offers some important additional advantage in terms of cell deposition accuracy and standardization as well as sophisticated and controlled production [87]. A 3D bioprinter platform developed by Pontiggia et al. consisted of modules for collagen and hydrogel blending, extrusion, and patterned inkjet dispensing of human skin cells to truly automate the manufacturing process of skin substitutes. By means of this bioprinting system, they were able to create large-scale, pigmented, prevascularized human dermo-epidermal skin substitutes (DESS) that could be easily handled by clinicians. They used fibroblasts, keratinocytes, melanocytes, blood endothelial cells, and lymphatic endothelial cells derived from human skin as well as a preclinical animal model to demonstrate its functionality *in vitro* and *in vivo* [88]. Liu et al. employed extrusion-based bioprinting to fabricate simple, robust full-thickness skin constructs by using sterile wire mesh through air–liquid interface culture. The ratio of bioink components, 3D model design, and printing conditions were optimized, and early constructs were built up for fibroblasts with sequential deposition of laminin and keratinocytes. The incorporation of laminin solution and seeding of epidermal cells followed by air–liquid interface culture enabled the production of full-thickness skin [89]. Li et al. prepared anovel cell-free 3D bioprinted wound dressing through photocroslinking gelatin/silk fibroin (SF) composite hydrogel which was then loaded with UiO-66(Ce) (MB@UiO-66(Ce)/PH) NPs and methylene blue (MB) (Fig. 2a). The wound areas in all five groups exhibited healing over time, as shown in Fig. 2b. Notably, the hydrogel groups consistently had smaller wound areas compared to the CON group at any given point after the operation. This trend was also supported by simulation graph (Fig. 2c) and data statistics (Fig. 2d). Additionally, in comparison to the control group, the hydrogels showed superior healing results and significantly reducing the time required for wound healing. Furthermore, applying PH-1 for 7 days successfully repaired full-thickness skin defects in mice [90].

Fu et al. conducted a study to explore the practical use of a 3D-printed skin substitute. They used a novel biomaterial that was loaded with human adipose-derived stem cells (hADSCs) and evaluated its effects on wound healing. To enhance the printability of the dECM pre-gel, a GelMA-HAMA polymer solution was incorporated.

This scaffold structure had the ability to expedite wound healing, facilitate collagen deposition, enhance re-epithelialization, reduce the inflammatory reactions and enhance healing quality through raising blood perfusion and encouraging angiogenesis [91]. Recombinant human collagen type III (rhCol3) was introduced by Yang et al. as a bioactive component to create a bioink for bioprinting human full-thickness skin equivalents. They used GelMA-rhCol3 composite bioinks to encapsulate human dermal fibroblasts. Then, they seeded human epidermal keratinocytes onto the encapsulated fibroblasts to form the dermis layer. The researchers found that higher concentrations of rhCol3 promoted proliferation of both cell types and accelerated healing skin wounds [92].

Despite advances in 3D skin bioprinting, the regeneration of hair follicles in areas with skin defects remains a significant challenge worldwide. Recently, Wu et al. offered a new insight and method to reconstructing complex skin appendages using bioprinting and inorganic bioinks. They developed a bioink consisting of calcium molybdate nanoparticles containing macrophages and dermal papilla cells (DPCs). Molybdenum in multicellular bioinks containing calcium molybdate nanoparticles was shown to polarize macrophages to the M2 phenotype and secrete anti-inflammatory cytokines. Furthermore, the scaffold's anti-inflammatory properties stimulated the release of cytokines associated with hair growth in DPC hair follicles, leading to the promotion of hair regrowth *in vivo*. Activation of mammalian target of rapamycins signaling in macrophages and the regulation of growth factors by molybdenum has been found to expedite the transition of hair follicles into anagen phase [93]. Kang et al. demonstrated a gelatin/alginate hydrogel (GAH)-based 3D bioprinting technique for constructing multilayered composite scaffolds that simulate the *in vivo* hair follicle microenvironment. To facilitate *in vivo* cellular processes, DPCs-laden GAH were dot-

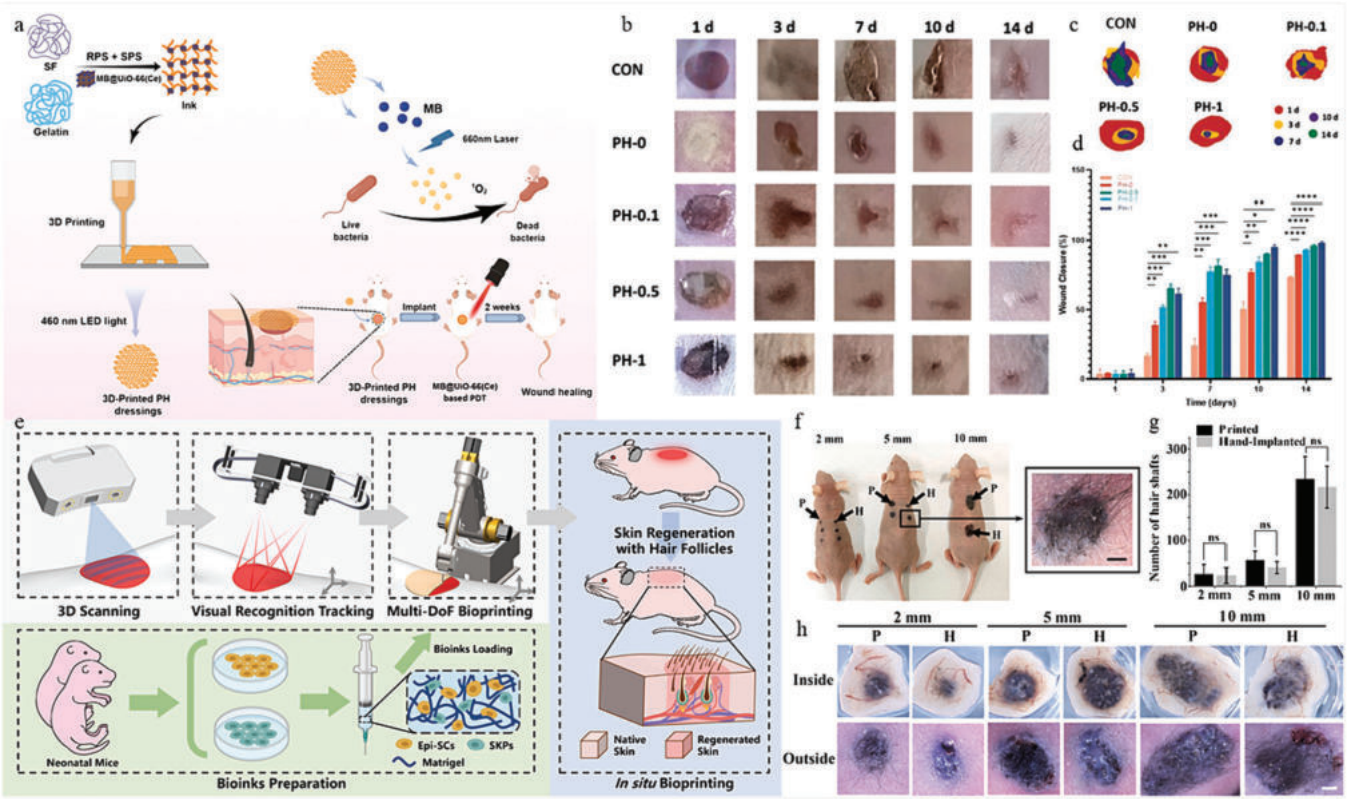

Fig. 2. (a) Schematic illustration of the design strategy and applications of a 3D bioprinted photocrosslinked hydrogel of SF/gelatin for full-thickness skin wound repair; (b) Illustrations of the hydrogel-treated incisional skin wounds at a specific time; (c) Simulation of the corresponding wound; (d) Quantitative analysis of wound site progression rates in different groups; (e) Workflow of an adaptive multi-degree-of-freedom in situ bioprinting robot for mice skin repair; (f) Generation of hair follicles within 4 weeks following the robotic bioprinting and manual implantation process; (g) The total number of hair shafts found in each group and wound; (h) Skin regenerated inside & outside. Reproduced with permission from Refs. [90,95] Copyright 2022, 2023 Whioce Publishing Pte Ltd, and John Wiley & Sons Inc.

printed into the scaffold. This multilayered scaffold exhibited appropriate cytocompatibility and increased DPC proliferation potential. Additionally, it restored DPC genes associated with hair induction and promoted the formation of self-aggregating DPC spheroids [94]. Zhao et al. presented a successful method for skin regeneration that combines novel robotic technology and bioactive bioink. An in situ multi-DoF adaptive bioprinter robot, consisting of a binocular vision system, a six-DoF controller, and scanning system was used in this study. This robot was utilized to conduct in situ bioprinting using skin-derived precursors (SKPs) and epidermal stem cells (Epi-SCs) obtained from neonatal mice and Matrigel was used as the bioink for skin repair. The process is depicted in Fig. 2e. Following bioprinting, the excisional wounds exhibited full healing and regeneration of functional skin tissue. The blood vessels, dermis, epidermis, sebaceous glands, and hair follicles of the regenerated skin closely resembled those of native skin, as shown in Fig. 2f–h.

3.2. Bone

Bone is an intricate composite of bioceramics and connective tissues that can produce blood cells, store minerals, as well as form the skeleton to support and protect the organs of the body [96]. Its hierarchical architecture comprises different levels: macrostructures (cortical bone and cancellous), microstructures (trabeculae), submicron-structures (lamellae), and nanostructures (embedded nanocrystalline minerals and collagen fibers). These structures contribute to providing mechanical function, supporting cell activities and facilitating mass transport. During active mass transfer between the inside and outside of bones, nutrients, oxygen, waste products, and blood cells are transported by highly vascularized bone tissues and the periosteum. Bone exhibits an inherent self-healing capacity that, however, is typically limited [97]. Disease, trauma, surgical resection, and congenital bone conditions can affect the strength and function of the bones, requiring regeneration and reconstruction via customized replacements (grafts) [98]. Although common transplantation techniques, including autografts and allografts, still remain the main solutions for regenerating bone defects, they are associated with some drawbacks. The use of autografts is invasive, costly, stressful to the patient due to the need for haervesting surgery, and may cause an infection that impacts both the donor and the surgical sites. Allografts also pose some problems such as potential immune rejection, infectious pathogenesis, and reduced osteoinductivity [99]. Therefore, bone regeneration via bone TE appears as an attractive alternative and, specifically, 3D printing/bioprinting is poised to influence this field. 3D bioprinting of bone tissue is expected to fabricate sophisticated hierarchical structures to biomimetic native bone tissues with high mechanical properties and also to meet the requirement that large tissue substitutes be vascularized to enable bone regeneration [100].

In this regard, a 3D bedside-bioprinting technique was used to create an autologous bone scaffold that was employed for cranioplasty. A polycaprolactone shell was designed to mimic the structure of the skull and function as the outer layer. In order to mimic cancellous bone for bone regeneration, 3D-printed autologous bone and bone marrow-derived mesenchymal stem cell hydrogels (BMSCs) were used. The results from the *in vitro* experiments demonstrated that the scaffold had a high affinity to cells and encouraged the transformation of BMSCs into bone cells in both 2D and 3D culture systems. Afterwards, the scaffold was implanted into cranial defects in beagle dogs for 9 months. During this time, it stimulated the growth of new bone and osteoid. Additional *in vivo* studies revealed that native BMSCs were drawn to the defect

while the transplanted BMSCs differentiated into vascular endothelium, cartilage, and bone tissues [101].

On the other hand, 3D bioprinting has the potential for effective vascularization in newly formed bone tissue for treating large bone defects. To repair bone defects, Shen et al. employed a 3D in situ bioprinting technique to successfully fabricate biologically active vascularized tissue bone (Fig. 3a). 3D bioprinted scaffolds containing bone mesenchymal stem cells were bioprinted with vascular endothelial cells laden in thermosensitive bioink (Fig. 3b). A coupling effect between osteogenesis and angiogenesis was demonstrated *in vitro* using the in situ vascularized scaffold (Fig. 3c). Furthermore, these scaffolds demonstrated outstanding performance in enhancing the growth of new bone in rat calvarial critical-sized defect models (Fig. 3d-f) [102]. Li et al. [103] successfully developed deferoxamine (DFO) (Eth)-loaded ethosomes in combination with a GelMA/gellan gum methacrylate (GGMA) hydrogel scaffold and a microcarrier-based sustained drug release strategy to print scaffold that mimics natural ECM equipped with the drug delivery system (Fig. 3g). By optimizing the bioink ratio and 3D bioprinting parameters, the composite scaffold's shape fidelity was maximized (Fig. 3h). Moreover, the controlled release of DFO could sustainably induce the migration and tubularization of HUVECs and the osteogenic effects of BMSCs (Fig. 3i). Consequently, this scaffold has the potential to trigger vascularization and osteogenesis, and help promote the regeneration of bones through activation of hypoxia-inducible factor 1-α (HIF1-α) signaling pathway providing a novel alternative for repairing bone defects [103]. The combination of 3D bioprinting with stem cells has great potential to facilitate cranial defect reconstruction. Nevertheless, due to the constrained cell behavior and functions, the scaffolds' efficacy has been hindered. Tao et al. conducted a study using a 3D bioprinting platform based on DLP technology to explore the potential of void-forming hydrogels in influencing the function of BMSCs encapsulated in GelMA/dextran emulsions for bone tissue regeneration. 3D bioprinted hydrogels stimulated YAP signal pathway, resulting in improved osteogenic differentiation of BMSCs. Moreover, it promotes the proliferation, migration, and spread of the encapsulated BMSCs. Void-forming hydrogel also showed promising results in delivering BMSCs and significantly accelerating bone regeneration, as demonstrated in *in vivo* therapeutic evaluations [104]. Epithelial-mesenchymal interaction (EMI), in addition, plays a significant role in bone regeneration. In this regard, Tang et al. combined dental papilla cells (DPCs) and HERS cells through 3D bioprinting to promote EMI and mimic the microenvironment of cell–cell interaction *in vivo*. In order to prepare two bioinks for 3D bioprinting, structural models of these two different types of cells were prepared using GelMA hydrogels. 3D bioprinted cell/GelMA constructs were implanted into Sprague-Dawley rats with alveolar bone defect. The findings showed that the 3D culture patterns produced a mineralized texture in HERS cells and DPCs, providing an ideal environment for promoting alveolar bone regeneration through their interaction [105].

3.3. Cartilage

Cartilage is a smooth, elastic connective tissue composed primarily of collagen fibers, proteoglycans, glycosaminoglycans, and high water

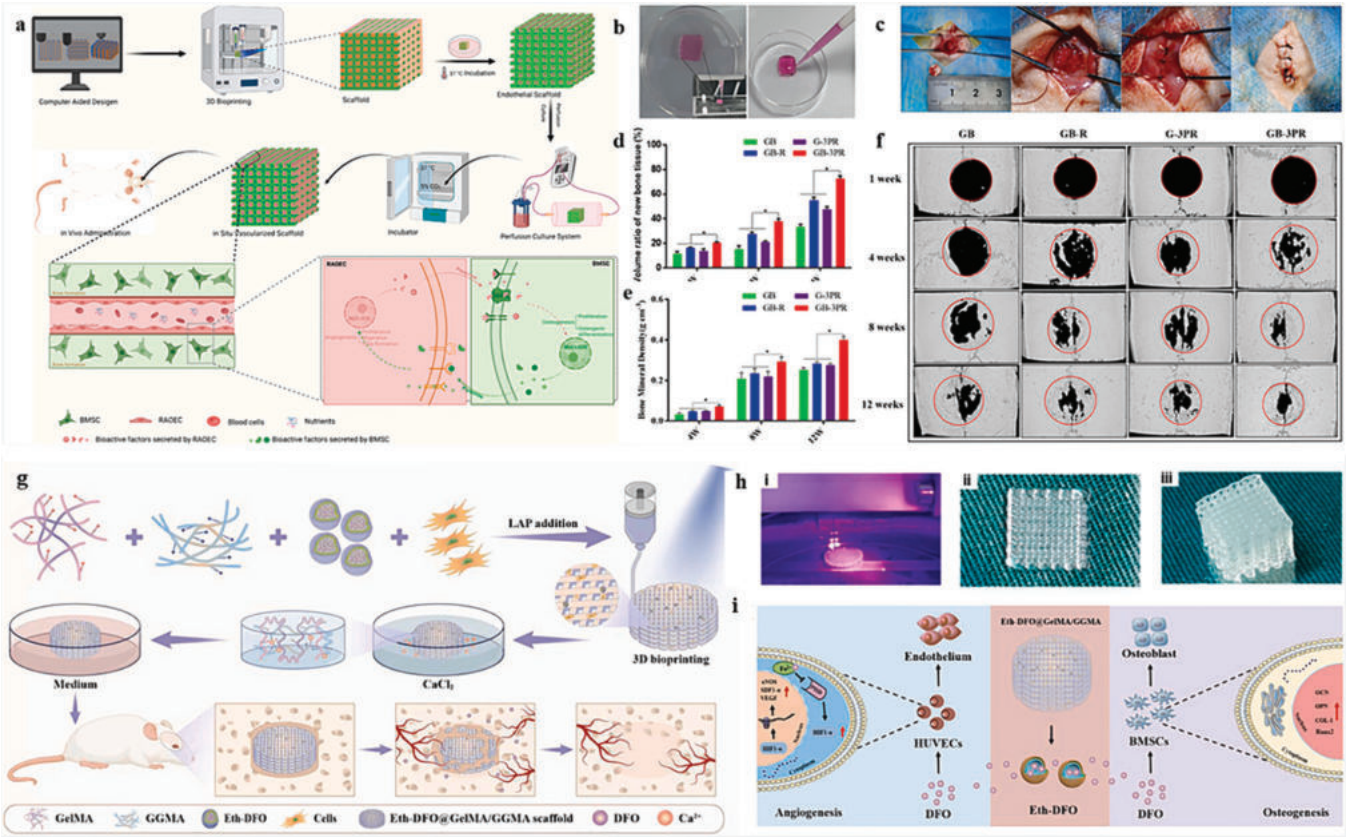

Fig. 3. (a) Schematic representation of the 3D bioprinting process for the creation of vascularized bone for the repair of bone defects; (b) Vascularized scaffolds printed in situ using BMSC-loaded GelMA bioink and RAOEC-loaded 3P bioink through two printing nozzles; (c) Isolation of the surrounding soft tissue to expose the skull and induce defects in a mouse model with critical pelvic size & insertion of the scaffold into the skull defect; (d) Quantitative analysis to assess newly formed bone tissue at the defect site; (e) Bone mineral density analyzed quantitatively; (f) Micro-CT analysis of the repair of a bone defect; (g) Schematic representation of the Eth-DFO@GelMA/GGMA scaffold bioprinting process; (h) Bioprinting of the GGMA 1% /GelMA1% scaffold: (i) printing process, (ii) Top-down view, (iii) 60-layer side view; (iv) Overview of the mechanism of osteogenesis and angiogenesis induced by EthDFO@GelMA/GGMA scaffolds. Reproduced with permission from Refs. [102,103] Copyright 2022 Elsevier Ltd.

content, and is found in the spine, ribs, synovial joints, nose, ears, and trachea; consequently, it plays a supporting in the body. Cartilage is formed during embryogenesis to serve as a template for bone growth and remains part of the mature skeleton [106]. It exists in the body in three main forms, including hyaline or articular cartilage, fibrocartilage, and elastic cartilage, with different relative contents of collagen II and proteoglycans, each of which performs specific functions [107]. It is a relatively simple tissue, devoid of nerves (aneural), lymphatics, and blood vessels (avascular), with low cell densities, primarily chondrocytes, that provide nutrients by diffusion. Spontaneous capacity for self-healing or regeneration of functional tissue defects is limited because of the inadequate supply and inherent non-proliferative nature of chondrocytes [108].

Common cartilage defects such as congenital anomalies, physical trauma, natural aging, and surgical interventions disrupt the biomechanical properties of joints, affect tissue function, and may lead to disability [109]. Today, the development of 3D bioprinting techniques allows producing well-controlled porous scaffolds with tissue-matched mechanical properties. 3D bioprinting from a variety of materials offers an unparalleled ability to deposit cell-laden cartilage constructs that mimic hetrogene structure and composition of native cartilage architecture [110]. For instance, Han et al. developed a hybrid ink through combination of PEGDA and ECM (Fig. 4a) containing BMSCs integrated with growth factors, which was employed in a high-precision electrowriting (EW) bioprinting technique to generate a highly-porous, hierarchical cartilage repair scaffold imitating the layered structure of native cartilage (Fig. 4b-e).

They evaluated the repair repair of femoral intercondylar cartilage injury in a rabbit model (Fig. 4f-i) by transplanting various scaffolds. These scaffolds successfully filled the annular cartilage injury between the rabbit's femoral condyles, as shown in Fig. 4i. In the control group without any treatment (BC), the cartilage remained unrepaired even after 24 weeks, indicating intrinsic difficulty in repairing cartilage damage. In the simple scaffold (SS) and composite scaffold (CS) groups, cartilage formation covering the lesion site was observed after 12 weeks. The CS group, however, demonstrated a significant repair effect at 24 weeks, with the cartilage completely covering the surface of the injured site and integrating well with the surrounding tissues. The cross-section also revealed successful regeneration of the cartilage [111]. Wei et al. designed and manufactured 3D-plotted cartilage scaffolds using a combination of sodium alginate/PVA precursors to be deposited layer-wise on a layer-by-layer platform. The result was a porous 3D hydrogel scaffold with an optimal pore structure that promoted chondrocyte proliferation [112]. Beketov et al. used extrusion bioprinting to print *de novo* cartilage using a bioink containing 4 % collagen and primary chondrocytes. *In vivo* results confirmed that the bioink successfully formed cartilage within 5–6 weeks after implanting the subcutaneous scaffold [109].

To highlight the the construct's architecture which resembles collagen II aggregates in natural tissue, Chakraborty et al. fabricated biomimetic arcuate structures of cartilage tissue through 3D bioprinting using two bioinks, GelMa and silk fibroin gelatin (SF-G). SF-G and GelMA both demonstrated the potential for chondrogenesis. However, compared to GelMA constructs, the bioprinted SF-G constructs showed increased proliferation of the human bone marrow mesenchymal stem cells that was encapsulated [113]. Pei et al., in another study, described a 3D bioextrusion printing technique to create a scaffold for cartilage repair, accurately imitating the surface of cartilage and its underlying

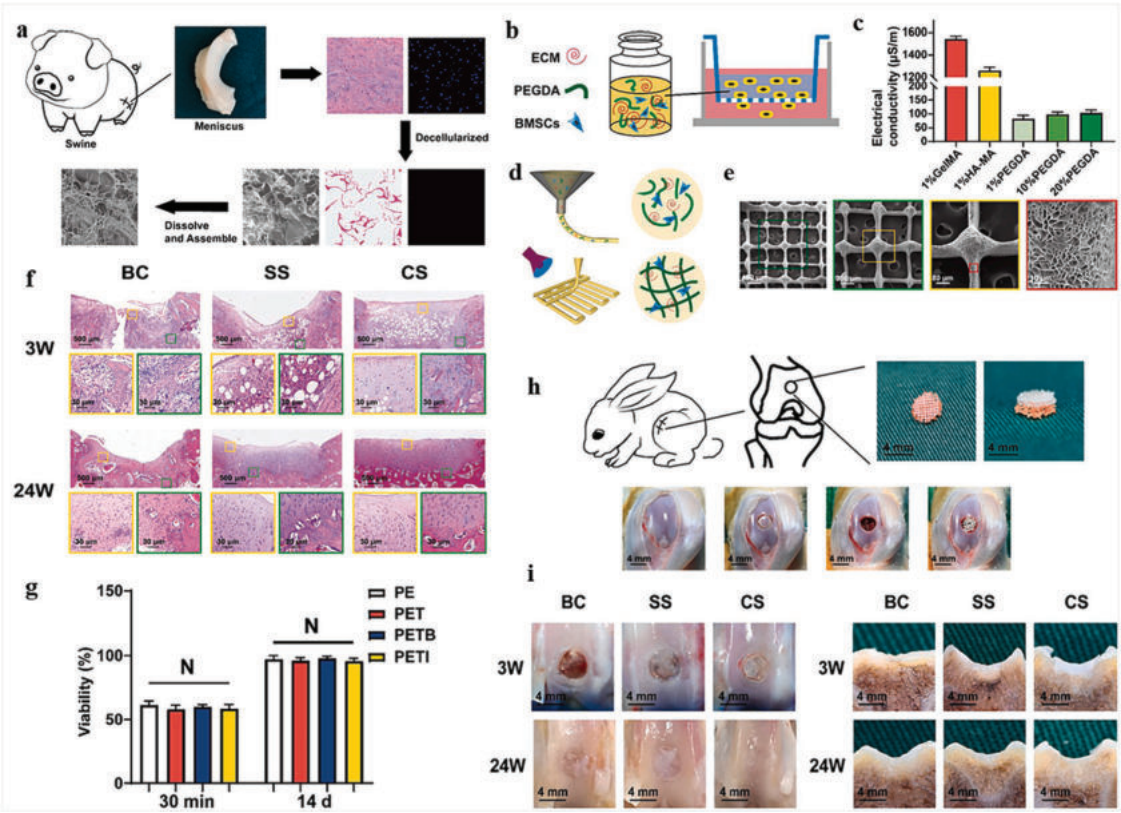

Fig. 4. (a) Production & morphology of ECM of swine meniscus examined using various methods (Such as observing the meniscus through a gross view, analyzing microscopic appearance, SEM images, and staining with HE and DAPI); (b) Schematic representation of the cell invasion experiment using Transwell; (c) Conductive characteristics of Gel-MA, HA-MA, and PEGDA; (d) Schematic representation of EW and photocrosslinking of hydrogel; (e) PEGDA/ECM hydrogel scaffold SEM image; (f) HE staining images of the blank control group (BC), simple scaffold group (SS) and composite scaffold group (CS); (g) BMSC viability at 30 min and 14 d after being printed on the scaffolds; (h) Schematic illustration of an animal experiment & an overview of the surgical procedure; (i) Cross-sectional & gross views of the BC, SS, and CS group 3 & 24 weeks following scaffold implantation. Reproduced with permission from Ref. [111] Copyright 2022 Elsevier Ltd.

subchondral tissue to provide an optimal microenvironment for repair. The study revealed that the fabricated GelMA-MSCs scaffold exhibited excellent biocompatibility and appropriate physicochemical properties. It also enhanced cell migration, proliferation, and chondrogenic differentiation. *In vivo* studies have further confirmed the effectiveness of the 3D bioprinted scaffold in promoting the regeneration of cartilage collagen fibers. This scaffold has shown significant impact in repairing cartilage in a rabbit cartilage injury model [114].

The tissue-based auricular reconstruction using polymer scaffolds has faced challenges in terms of clinical efficacy. While this approach has shown promise in early clinical trials. One of the main challenges is the potential for inflammation and deformation of the reconstructed structures. To address these challenges, Jia et al. presented a new approach for creating biological auricular equivalents with excellent mechanics and precise shapes using a special bioink composed of GelMA, polycaprolactone (PCL), and poly(ethylene oxide) (PEO), along with methacrylate-modified acellular cartilage matrix (ACMMA). To mimic the intricate microenvironment of cartilage and its cellular behavior photocrosslinkable ACMMA was used, while GelMA, PEO, and PCL were utilized to achieve a balance between printability and physical properties, ensuring precise structural stability, formed the microporous structure to allow unrestricted nutrient exchange, provided mechanical support for higher shape fidelity, respectively. The distribution of chondrocyte-loaded bioink, multi-nozzle 3D bioprinting technology, and PCL enabled the successful creation of microporous auricular equivalents. These equivalents have precise shapes and satisfactory mechanical strength. The most significant finding was the successful regeneration of mature auricular cartilage tissue in naked mice, which showed a high level of accuracy in terms of its shape, excellent flexibility, a large number of cartilage spaces, and the deposition of cartilage-specific ECM [115]. On the other hand, the polymer scaffolds used in tissue-based auricular reconstruction may not provide the necessary biomechanical properties and structural integrity required for a natural-looking and functional ear. Over time, the reconstructed structures may deform or lose their shape, further impacting the overall outcome. To overcome this issue, Zeng et al. incorporated bacterial nanocellulose (BNC) into GelMA hydrogel to improve the hydrogel's biomechanical characteristics and printability. The addition of 0.375 % BNC significantly improved the mechanical properties of the hydrogels and promoted cell migration within the BNC-enhanced hydrogels. In nude mice, the bioprinting of structures using chondrocyte-rich BNC/GelMA hydrogel bioink led to production of mature cartilage with higher glycosaminoglycan content and Young's modulus. Eventually, they successfully developed an auricle equivalent *in vivo*, which possessed precise geometry, advanced mechanics, and a rich cartilage-specific matrix [116].

nd DAPI); (b) Schematic representation of the cell invasion experiment using Transwell; (c) Conductive characteristics of Gel-MA, HA-MA, and PEGDA; (d) Schematic representation of EW and photocrosslinking of hydrogel; (e) PEGDA/ECM hydrogel scaffold SEM image; (f) HE staining images of the blank control group (BC), simple scaffold group (SS) and composite scaffold group (CS); (g) BMSC viability at 30 min and 14 d after being printed on the scaffolds; (h) Schematic illustration of an animal experiment & an overview of the surgical procedure; (i) Cross-sectional & gross views of the BC, SS, and CS group 3 & 24 weeks following scaffold implantation. Reproduced with permission from Ref. [111] Copyright 2022 Elsevier Ltd.

3.4. Skeletal muscle

Skeletal muscle accounts for approximately 45 % of adult human body weight and they play a variety of roles in skeletal support, locomotion, stability, and dynamic events such as metabolism regulation. They consist of muscle fibers that are wrapped by a thin connective tissue called endomysium. These fibers are aligned axially and grouped in a bundle, which is further protected by another connective tissue called perimysium. Several bundles are organized together to form a muscle, which is then covered by the epimysium. As well as being connected to the vascular system for receiving nutrients and eliminating waste, skeletal muscles are connected to the neuronal system for activation and contraction, and to the bones through tendons [117,118]. Muscle damage caused by trauma or tumor ablation impairs the function of the musculoskeletal system. Volumetric muscle loss (VML) injuries, which occur when more than 20 % of muscle mass is lost due to injury or surgical resection, are a debilitating orthopedic condition. This condition leads to permanent loss of muscle mass and function, resulting in long-term impairments and disability. Autologous muscle flap transfer is currently considered gold standard treatment for VML injuries. However, this treatment often leads to complications at the donor site, uneven muscle integration, and inadequate restoration of strength. Additionally, the fusion of muscle fiber bundles enhances the generation of force and enables directional movement in naturally occurring skeletal muscles that possess a well-organized structure.Therefore, the biofabrication of anisotropic biomimetic scaffolds which replicate the aligned structure of native skeletal muscle and promote cell elongation in a 3D environment, proves valuable for developing *in vitro* skeletal muscle models and preventing VML *in vivo*. To regenerate skeletal muscle tissue, the utilization of 3D bioprinting is anticipated to be a promising strategy and tool [118,119].

In order to print an anisotropic biomimetic scaffold for constructing *in vitro* 3D skeletal muscle tissue models and *in vivo* VML repair and, Li et al. used the printing gel-in-gel technique. By combining fibrinogen (FG) and GelMA, they developed an interpenetrating network (IPN) hydrogel with adjustable stress relaxation properties (Fig. 5a, b). Myoblast-loaded FG IPN viscoelastic hydrogel bioprint aligned 3D scaffold culture results demonstrated that this scaffold is capable of aligning and elongating control 3D myoblasts *in vitro*. In addition, the 3D bioprint-aligned scaffolds made from stress-reduced FG IPN hydrogel not only reduced stress but also created a microenvironment that facilitated the recruitment of innate cells. This microenvironment played an important role in promoting skeletal muscle regeneration after VML (Fig. 5c-e) [120]. Fornetti et al., in another study, developed a novel extrusion-based 3D bioprinting system exploiting PEG-Fibrinogen (PF) and its application to treat VML damage in mic model. This system has impressive biocompatibility *in vivo*, high efficiency in differentiating and organizing skeletal muscle cells *in vitro*, as well as high resolution of the printing fibers (~100 μm). The results demonstrated that this novel printing method has the potential to create *in vitro* biological replicas with well-organized muscle fibers that were able to contract independently and serve as a biological testing ground for myopathy research and drug development. Furthermore, the successful use of the printed construct to repair a VML injury in a mouse model, using both murine and human-derived muscle cells, suggests that this approach could be a valuable tool in regenerative medicine [121].

To investigate how myoblasts arrange and differentiate under different spatial constraints, as well as the impact of confined printing on skeletal muscle during maturation, Fan et al. utilized 3D bioprinting to engineered muscle-like bundles of varying widths using a simplified bioink system consisting of 3D printed fibrinogen and gelatin. In a fibrin hydrogel system, the C2C12 cell's fusion, alignment, differentiation, and maturation processes were observed. These results indicated that myotube differentiation was more pronounced in the thinner 3D bioprinted muscle-like bundles. Thus, they believed that the width of structures and the forces generated influence muscle fiber alignment and maturation [122]. Ronzoni et al. conducted a study to investigate the impact of various hydrogels on proliferation, differentiation, and viability of mouse myoblasts (C2C12) that were encapsulated in 3D bioprinted structures designed to support muscle regeneration.nThey performed the comparative study on three different hydrogel bioinks that are commercially available: (1) alginate and GelMA crosslinked with UV light, (2) GelMA, alginate-fibrinogen, and xanthan gum, and (3) alginate-fibrinogen/nanofibrillated cellulose (NFC) crosslinked with

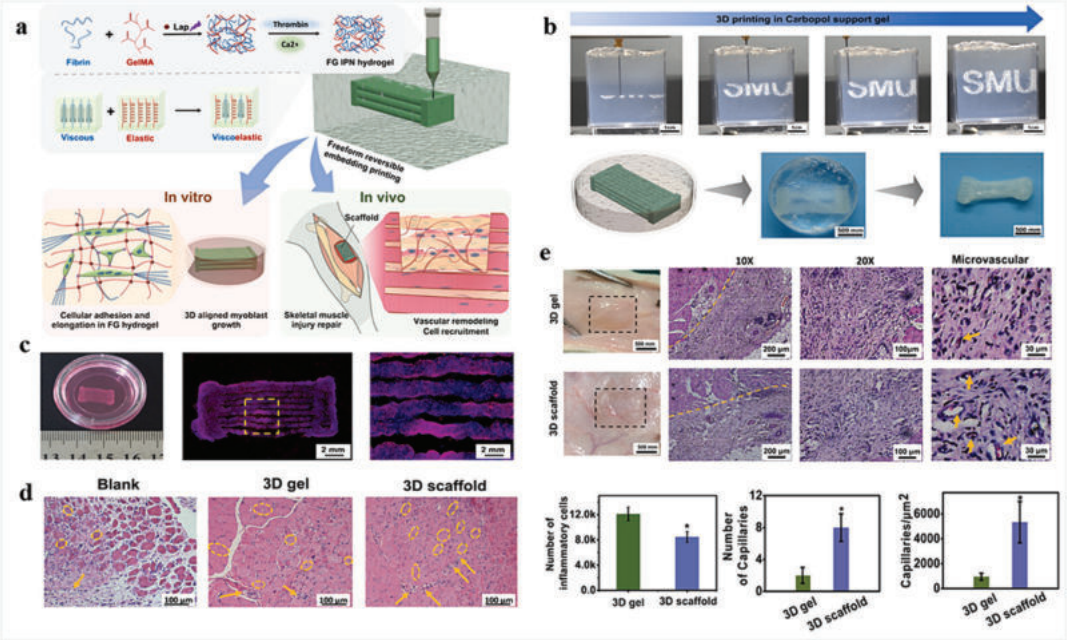

Fig. 5. (a) Schematic representation of fabrication process for a stress-relaxed FG IPN hydrogel-based 3D biomimetic bioprinting scaffold; (b) Schematic & procedure for printing 3D-aligned skeletal muscle scaffolds; (c) Images of C2C12 cells stained with F-actin and DAPI after 7d of culture; (d) Repair of skeletal muscle injury following implantation of the 3D aligned scaffold in a rat model over 2 weeks (The yellow circle indicates centronuclear myofibers and the arrowed circle represents microvessels) (e) Inflammation & angiogenesis after being implanted for 14d, as well as quantitative analysis to determine the number of inflammatory cells, generated capillaries, and capillary density in both the implanted 3D gel region & the aligned 3D scaffold group at day 14 post-surgery. Reproduced with permission from Ref. [120] Copyright 2023 Elsevier Ltd.

thrombin and calcium chloride. Among various studied bioinks, it was found that all constructs exhibited viability, proliferation, and differentiation. However, when NFC/alginate fibrinogen-based hydrogels were used, the stability of embedded myoblasts decreased significantly after 7–14 days in culture. The best results were obtained when they fused and initiated the growth of multinucleated myotubes. The results also indicated that myotubes were extensively aligned within hydrogel's linear structure. This alignment demonstrated improved myogenesis and cell maturation [123].

3.5. Tendon

Tendons and ligaments, which connect muscles to bones via fibrous collagenous connective tissues, are crucial for maintaining joint stability and enabling efficient load transfer between musculoskeletal tissues. Tendon injuries can compromise tissue integrity and reduce the ability to load-bearing. Unfortunately, these injuries have limited healing capabilities because tendons lack blood vessels and cellularity [124,125]. Despite significant progress in TE for tendon repair, treating tendon injuries remains challenging as current therapies fail to restore tendon function after injury. The replication of mechanical and biological heterogeneity of tendon and ligament is particularly challenging due to the intricate structures of such connective tissues [126,127]. 3D bioprinting is a desirable techniquefor biofabrication that allows for the creation well-organized scaffolds with precise pore sizes and geometries. This technique also enables better simulation of mechanical and biological properties of natural tendons and ligaments.

For example, Gottardi et al. achieved engineered constructs with spatially distinct cartilage and tendon components that mimic several aspects of the tendon-fibrocartilage interface at the tendon-bone attachment and could support cell survival, differentiation, and proliferation. They utilized a differentiation system based on a 3D-printed scaffold made of a highly biocompatible and superelastic material called PLGA. This scaffold had a microporous structure, with aligned fiber orientation on one side to mimic tendons, and a heterogeneous fiber organization on the other side to mimic cartilage. An advanced biphasic bioreactor system was used to culture the scaffolds in order to expose both sides to a differentiation medium simultaneously. The results confirmed that the engineered construct consisted of a side that resembled a tendon and a side that resembled cartilage. This construct has the potential to be used for surgical tendon repair after mechanical stimulation, in order to assess its withstand tensile stress. This is an important factor to consider before proceeding to *in vivo* models [128]. In another study, Jiang et al. introduced a novel strategy for rotator cuff tendon repair using multilayered PLGA scaffolds combined with collagen-fibrin hydrogels and adipose-derived MSCs (hASCs). This scaffold effectively facilitated the growth, prolifration, and diffrentiation of hASCs into tendon cells. Moreover, *in vivo* biocompatibility was confirmed by subcutaneous implantation of multilayer scaffolds. As well as enabling the development of cellular scaffolds with artificial grafts that are anatomically accurate in terms of shape and size, 3D bioprinting also made it possible to deliver cells and/or biomaterials to injured tendons and ligaments effectively [129].

3D bioprinting technology opens the door to development of platforms for the fabrication, maintenance, growth, and analysis of 3D tissue models *in vitro*, as well as drug screening in the field of drug discovery and development. In this respect, Laternser et al. combined 3D bioprinting with novel microplates to automate the generation of 3D musculoskeletal tendon-like tissue for drug screening purposes. By employing 3D bioprinting, the dumbbell-shaped tissue models were created using layers of GelMA-based bioink and cell suspension. These models were fabricated on unique postholder cell culture inserts that were placed in 24-well plates. The study successfully demonstrated the ability to print co-cultures of muscle and tendon tissues. Prior to this, we created monocultures of muscle and tendon tissues that showed promising differentiation. In the co-culture condition, the muscle tissue differentiated between the posts adjacent to the tendon tissue, while tendon tissue developed around the two posts [130]. Besides, through projection-based 3D bioprinting technology, numerous hydrogel particles of various sizes could be rapidly generated at once with proper

modeling and tuning of the printing platform specifications. This method enables the printing and molding of microgels in a single layer, while also protecting the encapsulated factors by eliminates the need for repeated elution and the use of organic solvents. For example, GelMA microparticles containing platelet-rich plasma loaded with tendon-derived stem cells (PRP-TDSC-GM) were created using a projection-based 3D bioprinting technique and then injected into a rat model with tendinopathy to evalute their impact on tendon structure and function under chronic inflammatory conditions. The results showed that PRP-GM facilitated proliferation and differentiation of TDSCs, demonstrating a favorable biocompatibility profile for tendon repair [131].

An effective method to reconstruct the interfaces between soft and hard tissues is to use biomimetic multicellular scaffolds with bifunctional properties that can induce the regeneration of multilineage tissue. The ability of biomimetic strategies to meet the diverse physiological needs of different tissues has gained significant attention in the field of complex structure regeneration. These dual-functional biomimetic scaffolds not only promote the differentiation of tendon/bone-related cells into osteogenic and tenogenic lineages *in vitro*, but also facilitate integrated regeneration of tendon-to-bone interfaces *in vivo*. By using a bilayered spatial distribution of biomimetic inks containing Mo-silicate (MS) bioceramics and BMSCs/tendon stem/progenitor cells (TSPCs), Du et al. achieved a bionic simulation of tendon-to-bone interfaces (Fig. 6a). After 14 days of culture in biomimetic multicellular scaffolds, TSPCs showed expression of genes involved in tenogenic differentiation (MKX, COL1, BGN, TNC, and DCN), indicating their tenogenic differentiation activity (Fig. 6b,c). Moreover, the biomimetic multicellular scaffolds demonstrated a remarkable ability to enhance the integrated regeneration of tendon-to-bone interfaces *in vivo* (Fig. 6d, e) [132].

N); (c) Tenogenic markers (TNMD & COL1) of scaffold stained with immunofluorescent proteins after 14d of culture; (d) Illustrations of the tendon-to-bone interfaces 12 weeks after surgery (The tendon is represented by T, fibrocartilage by F, and bone by B); (e) Micro-CT images representation of *in vivo* promotion of rabbit rotator cuff tear repair (RCT) 12 weeks postoperatively. Reproduce with permission of Ref. [132] Copyright 2023 Wiley.

3.6. Dental

Teeth are complex tissues composed of hard tissue, dentin, and enamel, connected to bone by ligament tissue. The formation of teeth involves a series of interactions between mesenchymal and epithelial cells. EC play a key role in enema formation, while mesenchymal cells produce odontoblasts, dental pulp, and other differentiated cells required for periodontal ligament formation [133]. Tissues are organized in ordered and intricate spatial structures involving different types of cells and have different mechanical properties which result in a range of mechanical properties from soft to hard. Gingival inflammation destroys the connective tissue that supports the teeth (gingiva, alveolar bone, periodontal ligament, and root canals), leading to tooth loss [134]. To tackle this complexity, 3D bioprinting has been considered as a promising TE strategy. 3D bioprinting in dental TE enables for precise control over structure and composition to create patient-specific tissues by using data and images from MRI or CT. Precise deposition of cells, matrices, and signaling components enables the fabrication of sophisticated constructs [135]. It also enables the incorporation of growth factors and multiple cell types to promote tissue development. These complex constructs have the potential to revolutionize dental treatments and hasten the shift from conventional restoration methods to bio-engineered ones. Bioprinting offers a wide range of applications in dentistry such as orthodontic models, dental aligners, direct crowns and bridges, denture bases, night guards, flexible gingiva masks, and surgical drilling templates [135,136]. For example, to regenerate periodontal ligament, Lee et al. fabricated a 3D printed hybrid artificial organ using human periodontal stem cells (hPDLSC) to form a periodontal ligament on a titanium surface. Instead of using traditional cell seeding methods, the researchers used a cell-printing technique to create a periostin-positive connective tissue interface between the 3D printed titanium scaffold and bone. Animal experiments demonstrated an increase in connective tissue after implanting the hybrid artificial organ into a calvarial defect model. This incorporation of fibrous connective tissue between the titanium implant and the bone, near the oral mucosa, allows for the restoration of physiological tooth functions, such as the ability to respond to mechanical stimuli and resist infection. This technique can also be applied to reconstruct using a 3D printed hybrid artificial organ through bioprinting [137].

With the aim of creat 3D bioprinted dental construct that contained

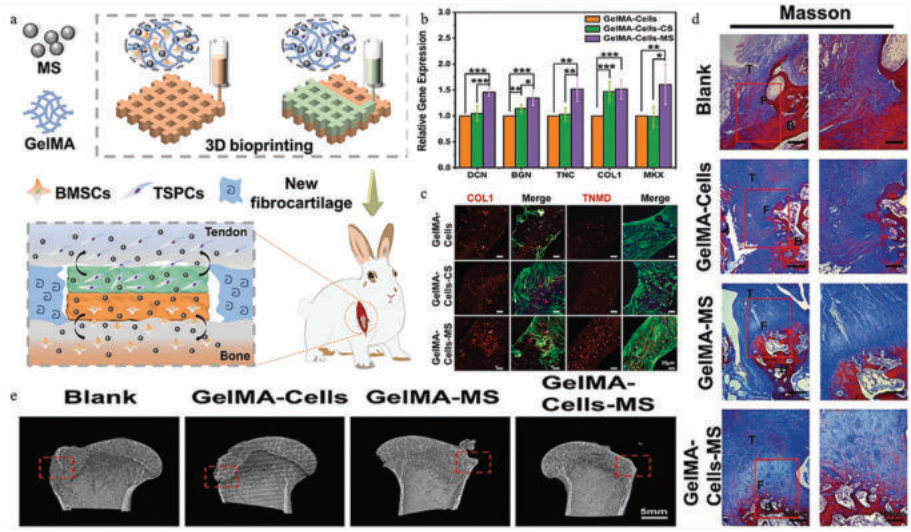

Fig. 6. (a) Schematic representation of biomimetic multicellular scaffold fabrication & application for reconstruction of tendon-bone interfaces; (b) Expression of genes related to tenogenic differentiation (MKX, COL1, BGN, TNC, DCN); (c) Tenogenic markers (TNMD & COL1) of scaffold stained with immunofluorescent proteins after 14d of culture; (d) Illustrations of the tendon-to-bone interfaces 12 weeks after surgery (The tendon is represented by T, fibrocartilage by F, and bone by B); (e) Micro-CT images representation of *in vivo* promotion of rabbit rotator cuff tear repair (RCT) 12 weeks postoperatively. Reproduce with permission of Ref. [132] Copyright 2023 Wiley.

human dental pulp stem cells (hDPSCs), Park et al. developed bioink formulation that incorporated a bone morphogenetic protein (BMP) peptide tethering system. The results demonstrated successful conjugation of a thiolated BMP-mimetic peptide into a GelMA-based bioink formulation. This bioink formulation accelerated hDPSCs' odontogenic differentiation while also promoting high viability and proliferation of the cells [138]. In another study, Han et al. developed a novel bioink using Human demineralized dentin matrix (DDM) particles (DDMp) and a fibrinogen-gelatin mixture for regeneration of patient-specific shaped 3D dental tissue (Fig. 7a). The bioink viscosity and shear thinning behavior gradually improved (Fig. 7b-e) with increasing DDMp concentration, enhancing printability of bioink (Fig. 7f). As DDMp content increased, printing resolution and stacking capacity also increased (Fig. 7g). Furthermore, DPSC odontogenic differentiation was significantly enhanced with increasing DDMp concentration (Fig. 7h) [139].

3.7. Cornea

Cornea is highly organized, dense, avascular, and transparent which protects eyes from the external environment and is responsible for incident light transmission and refraction. It has a specific arrangement of collagen fibers forming 200–250 lamellae, which give it strength and a spherical shape. The anterior part of the tissue's collagen lamellae are intertwined and aligned in the middle and posterior regions. The transmission and refraction of light, which then focuses on the retina, are caused by this particular alignment [89,140]. An important contributor to blindness globally is corneal disease. Currently, corneal transplantation is the most common treatment for corneal blindness. However, donations are the main source of corneal transplants, which is far from meeting the need. A critical shortage of donor corneas has prompted research into effective corneal replacements. Nevertheless, many questions remain that cannot be resolved by current research, including the restoration of optical function and reconstruction original geometry of the eye [141]. 3D printing allows the deposition of materials on digital command to construct results with sophisticated geometric patterns. Advances in 3D bioprinting technology are expected to allow for precise control of corneal curvature and thickness based on the specific refractive requirements of individual patients, overcoming the drawback of traditional TE [142].

Two major challenges for conventional corneal materials are rapid epithelialization and stable epithelial processes. These processes are attributed to the curvature of the cornea which plays an important role in determining the epithelial response to corneal damage and the corneal healing process. In a study by Xu et al., GelMA and collagen were utilized to generate smooth, 3D-printed convex corneal implants. These implants exhibited curved structures that could regulate cell organization and adhesion. The study divided the surfaces into four regions and examined how cells perceive topological cues on curvature, which are influenced by the distribution of epithelium and differences in adhesion in different regions of the natural cornea. The researchers discovered that seeding rabbit corneal epithelial cells (RCEC) on convex structures with a steep slope gradient resulted in more aligned cellular organization and stronger cell-substrate adhesion. This finding was further confirmed through finite element simulation and signal pathway analysis. Another factor that contributed to the increased density of adhesive molecules was the activation of genes and proteins involved in adhesion. The use of FEM analysis allowed for the simulation of tensile forces, which confirmed the observed increase in adhesion. When convex implants were transplanted *in vivo*, they demonstrated greater adaptability to adjacent tissues and stronger cell adhesion compared to planar implants. This resulted in accelerated corneal epithelialization within 180 days, as well as improved regeneration of collagen fibers and nerves. Taken together, the use of printed convex corneal implants that promote corneal regeneration could serve as a promising treatment strategy for corneal injuries [143]. In another study, Kim et al. calculated the wall shear forces exerted on the shear-thinning bioink during 3D printing. The results demonstrated that the shear stresses varied depending on the nozzle diameter, resulting in different distributions of collagen-fibril orientation. Furthermore, the researchers evaluated the application of these approaches to corneal remodeling by considering cornea-specific features such as the crisscross-patterned collagen fibrils and light transmittance. Over time, this structural regulation improved vital cellular processes involved in collagen assembly, and the collagen fibrils that underwent remodeling along the printing path produced a lattice

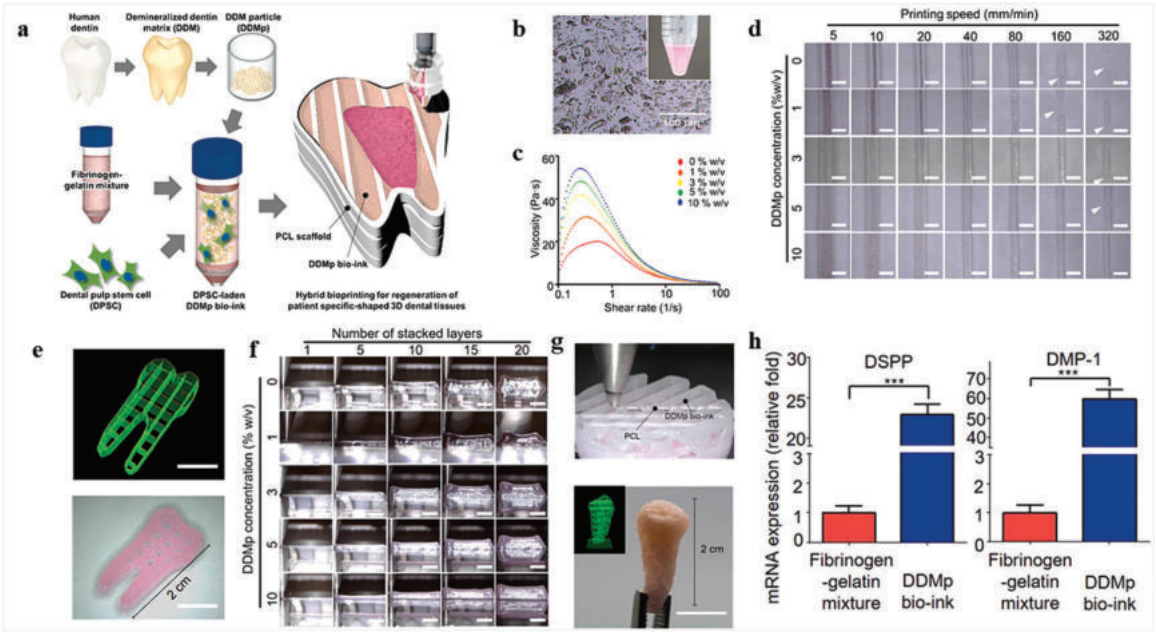

Fig. 7. (a) Schematic represents demineralized dentin matrix particle (DDMp) bioink preparation; (b) Microscopic image of a DDMp bioink; (c) Viscosity of the DDMp bioinks; (d) Microscopy image of DDMp bioink printability test; (e) Visual printing code & fabrication results of tooth-shaped hydrogel structures; (f) Microscopic image of the DDMp bioink stacking test; (g) 3D hybrid bioprinting process & visualized printing code; (h) Relative expression levels of dentin matrix-1 (DMP1) and dentin sialo-phosphoprotein (DSPP) mRNA. Reproduced with permission from Ref. [139] Copyright 2021 MDPI.

pattern resembling the natural structure of the human cornea [144].

For upcoming patients with corneal stromal diseases, the suggested bioprinted human 3D corneal models could potential to be used as transplantable constructs. In this regard, Duarte Campos et al. provided the bioprinting of 3D models of mimicked cornea fabricated through the freeform, cell-friendly drop-on-demand technique. These models were closely resembled the native corneal tissue and had similar optical properties, as confirmed by optical coherence tomography. Furthermore, the corneal stromal keratocytes that were bioprinted remained viable throughout the bioprinting process. They also maintained their natural dendritic shape and exhibited the phenotypes of keratocytes [145]. On the other hand, optimal topographical and biological environments to promote corneal regeneration can be provided by the synergistic effect of precisely positioned cells and microstructure. Few studies have used DLP to achieve curvature emulation corneal printing to accurately print different cell sources on different layers to regenerate both epithelium and stroma *in vivo*. For example, He et al. utilized GelMA/PEGDA-based 3D printing to fabricate a bilayer implant for corneal regeneration (Fig. 8a). High fidelity and robust surgical handling capabilities were achieved by printing out a bilayer dome-shaped corneal scaffold composed of an epithelial layer filled with rabbit corneal epithelial cells (rCECs) and an orthogonally aligned fibrous stromal layer filled with rabbit adipose-derived mesenchymal stem cells (rASCs) (Fig. 8b). By using a rabbit keratoplasty model and this bi-layer corneal scaffold, re-epithelialization, corneal defect sealing, and stromal regeneration were accomplished (Fig. 8c). The coordinated effects of the microstructure of the 3D printed corneal scaffold and the precise positioning of cells in the epithelial and stromal layers provided an optimal topographical and biological microenvironment for corneal regeneration. (Fig. 8d,e) [146].

3.8. Vascular and cardiovascular tissues

To maintain viability and functionality, most tissues of the human body possess complex branched internal vascular systems to meet their oxygen, nutrients, and growth factor requirements, as well as collect waste metabolites [147]. Regardless of vessel caliber, all vessels have a multi-layered structure comprising endothelium and endothelial cells, deposited over a basement membrane and typically containing type IV collagen, laminin, and integrins. Capillaries are distinguished by presence of the endothelium and basal membrane. However, larger and more mature blood vessels possess three additional layers of ECM. The tunica intima (the most internal layer) consists of endothelial cells, while the tunica media (middle layer) and the tunica externa (the most external layer) are consist of smooth muscle cells supported by elastic and collagenous connective tissues, which affect blood vessel mechanical properties [148].

The development of connected 3D vascular networks within tissue-engineered constructs has the potential to significantly improve the functionality and performance of engineered tissues. Therefore, considerable effort has been devoted to promoting angiogenesis *in vitro* to mimic the native vascular network for blood transport, mass exchange, and long-term tissue survival [149,150]. Although the ability to create vascular features with TE is often limited, 3D bioprinting holds promise for depositing predefined material components and cells to generate functional 3D vascular networks [151]. In this regard, Zhang et al. [152] converted a robotic arm with 6-degrees of freedom into a bioprinter in order to rapidly and accurately deliver multiple cell types from cell mixtures (Fig. 9a,b). Self-designed bioreactors and repeated printing and culturing strategies were also developed to better preserve natural cell functions (Fig. 9c). Hydrophobic forces between the water-based bioink and oil-based printing environment ensured cell

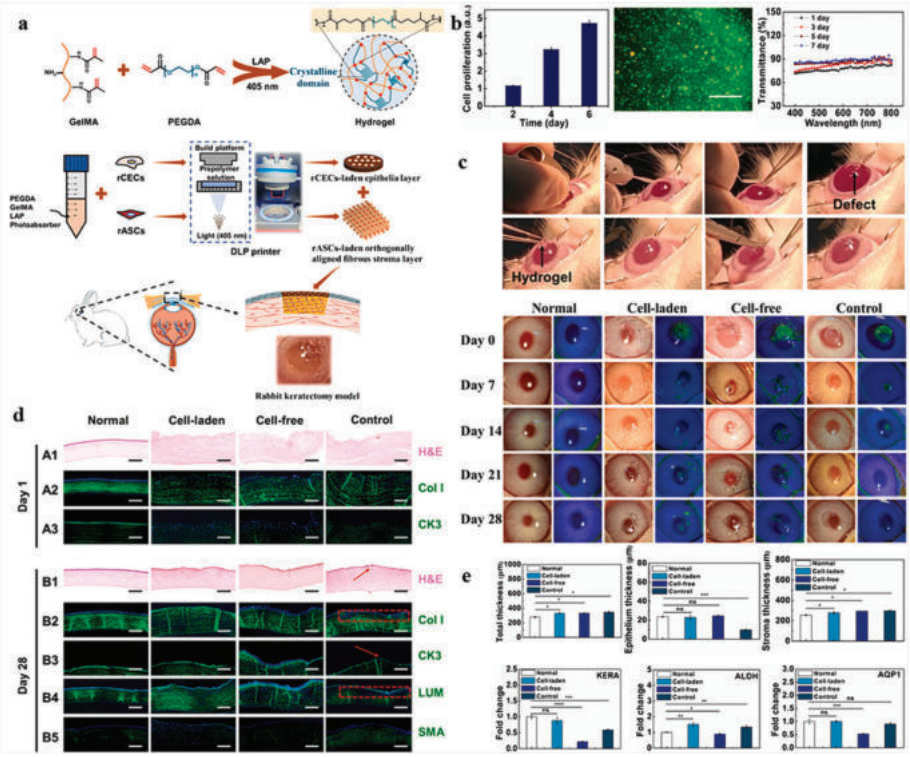

Fig. 8. (a) Schematic representation of PEGA-GelMA hydrogel formation & bioprinting procedure; (b) Cell proliferation, live/dead image, & change in transparency of rCEC-containing hydrogels; (c) *In vivo* evaluated the effectiveness of a corneal scaffold in a rabbit model (Gradual reduction in the size of the corneal epithelial defect, represented by the green area in the center of the cornea, was observed due to the migration of the epithelium on the hydrogel and the defect); (d) Gene expression & histological analysis (Red arrows and rectangles represent unfinished regions of epithelium & stroma, respectively; (e) Thickness of entire layer, epithelium, & stroma of the cornea and relative gene expressions of KERA, ALDH, AQP1 in the cornea (Values reflect fold changes in mRNA expression on normal corneas). Reproduced with permission from Ref. [146] Copyright 2022 Elsevier BV.

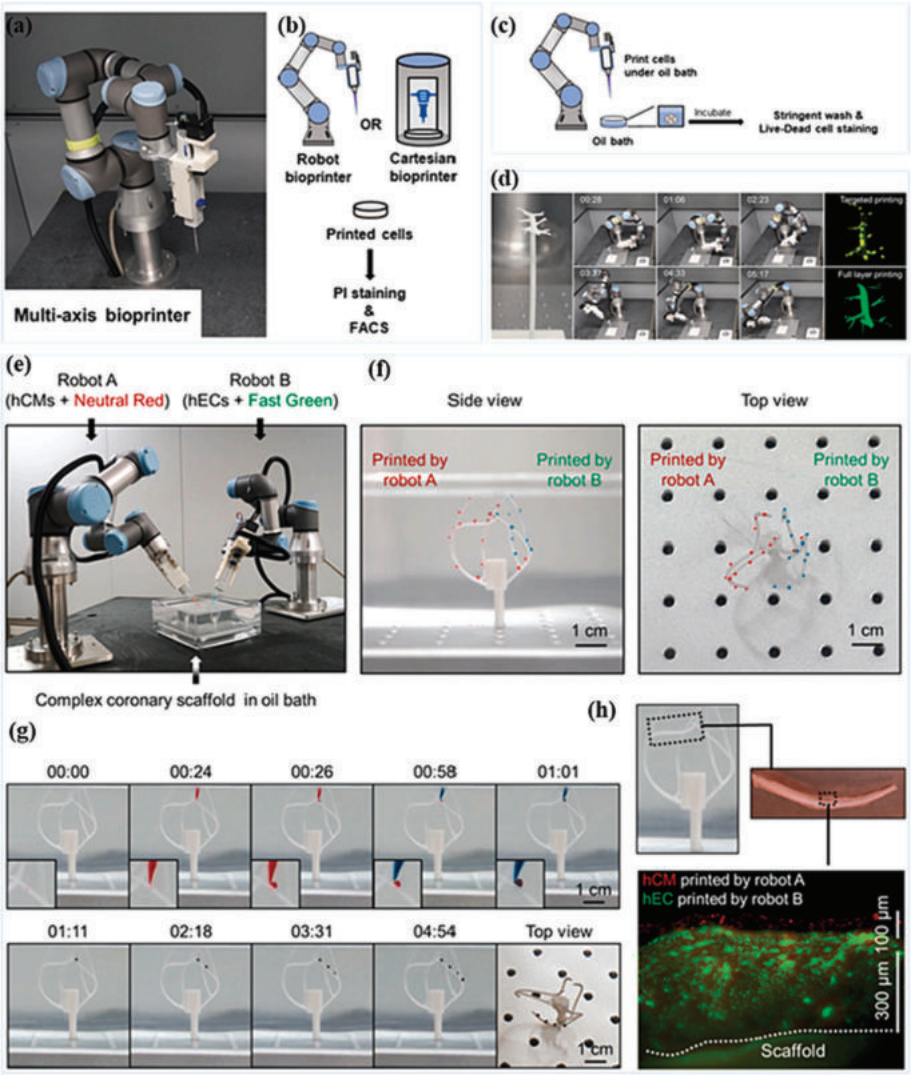

Fig. 9. (a) Configuration of 6-DOF robotic bioprinter; (b) Evaluation of the mechanical damage of cells printed; (c) Bioink screening for optimal cell concentration; (d) The printing of cells onto a complex vascular scaffold (left) and the final results (right); (e) Establishment of a two-robot bioprinting platform; (f) Side and top views of bioink printed on the scaffold; (g) Co-printing of bioinks at the scaffold position; (h) A co-printing robot-generated, well-organized hEC-hCM cell layer structure on a coronary scaffold branch. Reproduced with permission from Ref. [152] Copyright 2022 Elsevier BV.

attachment to the scaffolds. This strategy effectively maintained cellular function and promoted the development of vascular networks. To generate artificial blood vessels with vascular branches and *de novo* capillaries, angiogenic factors were included in the perfusion medium. In addition, this bioprinting system was capable of generating cardiovascular and contractile tissues with long-term survival (Fig. 9e-h) [152]. In light of the good elasticity and cell adhesion provided by modified electrospinning as well as increased stability during the printing process, which is given by modified traditional rotary bioprinting, Jin et al. [153] successfully constructed precellular small-diameter blood vessels (<6 mm) with the aid of these two cutting-edge technologies that possess the advantages of both techniques. This biomimetic blood vessel was constructed by electrospinning poly (ε-caprolactone) (PCL), bioprinting with GelMA-based bioinks containing smooth muscle cells (SMCs), and perfusing with HUVECs [153].

To ensure proper nutrition and oxygen delivery as well as efficient waste elimination, native capillary beds are structured and densely packed throughout metabolically active tissues. In a method that has significant implications for engineering microvascularized tissues, Jewett et al. introduced a method for creating scalable capillary networks with user-defined architecture combined with 3D cell-laden hydrogel constructs. By magnetizing both the lattice and ECs, two existing techniques were employed to create lattices made of sacrificial microfibers that could be uniformly and effectively seeded with ECs. By using fiber electropulling and solution electrowriting to create microfibers, ferromagnetic microparticles were incorporated. A bacterial lipase that did not affect functionality or viability of mammalian cells selectively degraded the capillary templating lattice after it enclosed in a hydrogel [154]. In order to promote neo-vascularization with tunable mechanical properties, Zhou et al. [155] employed a coaxial extrusion platform to fabricate novel GelMA/gelatin/sodium alginate-based biomimetic vessels. The results showed that by optimizing the hydrogel formulation, the mechanical properties of 3D-bioprinted vascular such as compressibility and elastic modulus could be tuned to withstand specific blood pressures found in real tissue [155].

The heart, the first functional organ formed during embryogenesis, has a stylized four-chambered muscular anatomy and responsible for continuous blood circulation throughout the body. A complex hierarchy and cellular diversity consisting of cardiomyocytes (CM), EC, fibroblasts, connective tissue cells, smooth muscle cells, and other specialized cells pose great challenges to the manufacturing of functional heart tissue [156,157]. Although 3D bioprinting cardiac tissue is still in the

early stages of exploration, recent researches have indicated the possibility of 3D bioprinting functional heart tissue, particularly customized cardiac valves, and patches [156,158]. However, such approaches have limitations in terms of full vascularization and synchronous contractile activity [159]. In this respect, Cetnar et al. [160] introduced a new generation of anatomically precise 3D functional patient-derived models at various stages that can be used as a high-fidelity and robust platform to study various cellular microenvironment interactions, comprising geometry, ECM composition, flow hemodynamics, and biomechanics under both dynamic and static flow conditions. Models of the human embryonic heart tube and fetal left ventricle were bioprinted using hydrogel-based seeded with endothelial cells, and analyzed both experimentally and computationally. Based on cardiac geometry and flow conditions, there was a great variation in endothelial cell proliferation and endothelialization in these bioprinted constructs. The results demonstrated a similar and precise flow hemodynamic pattern in the 3D space and within the bioprinted constructs [160]. By focusing on optimizing bioprinted cardiac patches, Roche et al. developed alginate/gelatin-based heart patches for myocardial regeneration, the results showed the presence of EC networks, which formed a durable structure and exhibited contractile function [161]. Polonchuk et al. successfully constructed functional cardiac spheroids (CSs) composed of ECs, fibroblasts, and human cardiomyocytes blended into an optimal alginate/gelatin hydrogel with viscoelastic properties comparable to native heart tissue. As a result of spontaneous contraction and stimulation of bioprinted CSs, it was possible to record electrical signals and contractile on microelectrode plates. Taken together, these results indicated that bioprinted CS has great potential to reconstitute human cardiac tissue for long-term *in vitro* studies [162].

3.9. Neural tissue

Undoubtedly, the neural system is the most intricate part of human anatomy and is composed of neurons, specialized cells with extensions (axons and dendrites) that transmit neuro-electrical signals throughout the body and perform a variety of tasks such as support neurological function and reparative effects in neurological and craniocerebral injury [163,164]. The nervous system comprises two neural networks: the central nervous system (CNS) which refers to the spinal cord and brain, and the peripheral nervous system (PNS) which contains neurons distributed throughout the body. Both of these function together respond to external stimuli and regulate homeostasis. Minor injuries to the PNS heal and regenerate spontaneously, while significant injuries need surgical treatment. The CNS, on the other hand, is much more complex and rarely recovers spontaneously [164,165]. 3D neural bioprinting could be a potential technique for generating new neural tissue or improving the innervation of tissue-engineered constructs that need to be integrated into the host's nervous system. Moreover, 3D bioprinting with its ability to manipulate multiple materials simultaneously and provide spatial patterns in the scaffold could be even more appealing in this field due to the intricate architecture and microenvironment of neural tissue [166,167]. The feasibility of neural tissue bioprinting from patient-derived mesenchymal stem cells (MSCs) was demonstrated in a study by Perez et al. [168], where adipose tissue-derived MSCs were successfully bioprinted by using fibrin-based bioink by employing RX1 microfluidic bioprinter. Characterization of neuronal tissue revealed high cell viability, Expression early neuronal marker class III beta-tubulin, and neuronal dopaminergic markers tyrosine hydroxylase and dopamine release. Furthermore, after exposure to potassium chloride, tissues exhibited immature electrical signals [168]. For enhancing nerve regeneration, Song et al. [169] developed a bioprinted scaffold using a hydrogel matrix consists of modified poly (3,4-ethylenedioxythiophene) (PEDOT), GelMA/PEGDA hydrogel matrix and neural stem cells (NSCs). This 3D bioprinted electroconductive hydrogel scaffold exhibited appropriate biocompatibility, good conductivity, and proper mechanical properties, which provide an optimal microenvironment for NSC growth, adhesion, and proliferation. Moreover, modification of the polyphenolic structure of PEDOT chains improves both the electrical properties of 3D electroconductive hydrogel scaffold and differentiation of NSCs into neurons [169].

Living nerve-like fibers, which have been 3D printed with optimized biological functions and reduced complexity, offer new and reliable methods for repairing spinal cord injuries. This advancement is crucial for the development of future clinical applications. For instance, Yang et al. successfully developed a living microtissue using extrusion-based 3D bioprinting. They utilized a native hydrogel that closely resembled the ECM. This hydrogel contained a high concentration of NSCs that were arranged in a spatial orientation similar to native nerve fibers (Fig. 10a). In vitro examination of these biofibers demonstrated that they provided a suitable environment for NSCs. The niche supported long-term cell viability, allowed for cell migration and proliferation, and differentiation into functional neurons. Additionally, the biofibers exhibited signaling abilities (Fig. 10b). To assess the potential of these nerve-like fibers in promoting neurogenesis, researchers conducted experiments using a rat model with a complete transected spinal cord injury (Fig. 10c). Transplanting living nerve-like fibers has been proven to improve the ecological environment of the damaged area by regulating the immune response, promoting blood vessel growth, generating new neurons, forming neural connections, and remodeling neural circuits. This leads to improved functional remodeling and provides insights into the evolutionary process of this living construct (Fig. 10d, e) [170].

On the other hand, an *in vitro* model of the neurovascular unit (NVU) is effective for studying brain function and drug development. Aiming reconstruction of a functional NVU model, Wang et al. presented a method to regulate stiffness of the tissue model, which had a microenvironment similar to the brain's ECM and multi-cellular hollow coaxial geometries. To fabricate 3D neurovascular constructs with a low modulus of ECM, they proposed a two-stage methodology. During shaping stage, a low-viscosity mixture of collagen/alginate was utilized and printed using an embedded method. In the culturing stage, they removed alginate by targeted lysing. Rapid crosslinking and low viscosity improved printing resolution, while the lysis process reduced the hydrogel's elastic modulus and tailored the microstructural porosity to provide an environment that mimicked the brain's ECM [171].

3.10. Liver

As the largest organ in the human body, liver is divided into the right and left lobes, which are separated through a band of connective tissue, that anchors it to abdominal cavity. Primarily liver is composed of vascular networks and the functional unit with a hexagonal structure called the hepatic lobules. The liver consists mainly of parenchymal hepatocytes, which are of endodermic origin. Other cells that compose liver include hepatic stellate cells (HSC), portal vein fibroblasts, stromal cells, Kupffer cells, sinusoidal endothelial cells (SEC), and biliary epithelial cells [172]. Liver performs vital functions such as urea synthesis, metabolism of fats, carbohydrates and proteins, detoxification, hematopoietic and coagulative functions [173]. In general, compared to other organs, the liver has a large capacity for self-regeneration. However, this regenerative ability is compromised when it is continuously and/or severely damaged by certain illnesses or injuries. While the exact causes for this reduced capacity are not completely understood, in many instances, the presence of severe scarring and fibrotic tissue will ultimately lead to liver failure, necessitating a liver transplant [174]. However, scarcity of healthy donors, surgical complications, the risk of rejection, and healthcare expenses limit the benefits of transplantation. Therefore, in recent years, various techniques, especially bioprinting of biomimetic liver tissues, have gained particular attention [175].

The primary constraint on the intricate spatial organization and cellular composition of liver tissue is the performance of bioink materials. The bioink material must meet both printability and bionic

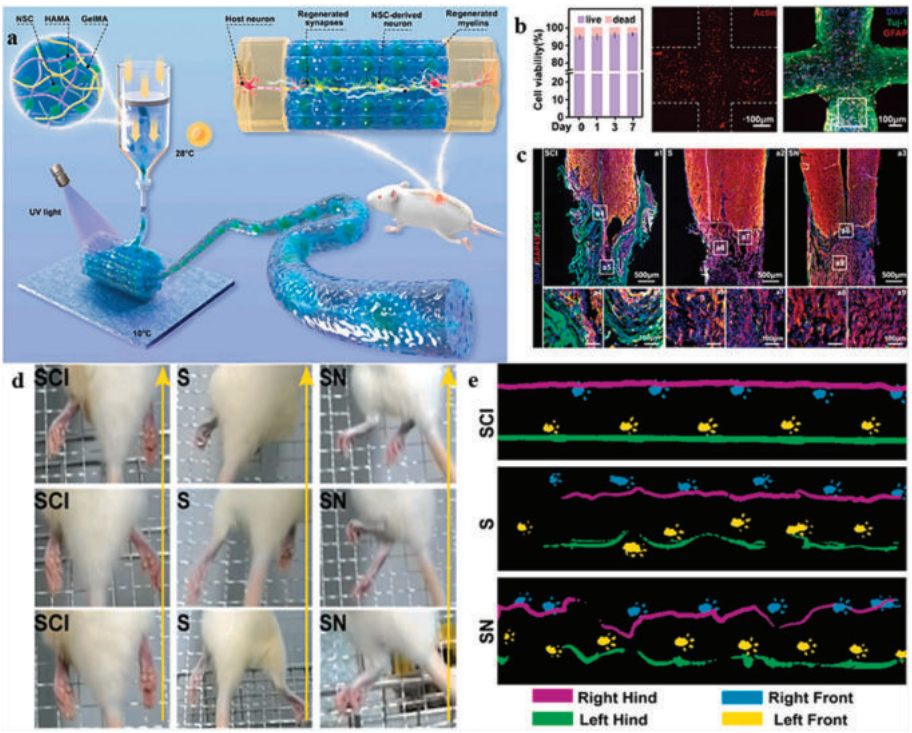

Fig. 10. (a) Schematic representation of the development of a functional network *in vivo* using 3D bioprinted living nerve-like fibers; (b) The staining image of bioprinted NSC-loaded scaffolds and the cell viability of the scaffolds; (c) Immunofluorescence images of living nerve fibers creating a suitable environment for neonatal neurons, with enlarged images of specific markers (DAPI (blue), GAP43 (red)) and CS-56 (green) (a4–a9) are the images enlarged by (a1–a3)); (d) Sequential images of rat hind limbs climbing from the bottom, indicated by upward-pointing arrows; (e) Footprints recorded by the Catwalk system. Reproduced with permission from Ref. [170] Copyright 2023 Elsevier BV.

requirements for different cell types and ECM. To mimic cellular heterogeneity, ECM features, and spatial structure, Jian et al. reported a method for 3D bioprinting liver organoids with biomimetic lobular structures using multicellular droplets. To guarantee structural integrity and offer flexible designability, sodium alginate-based bioink 1 and dipeptide-based bioink 2 were utilized, respectively. After 7 days of culture, the liver organoids could maintain their cellular distribution and structural integrity within the printed lobule-like structure. The created 3D organoids exhibit high levels of cell viability, urea synthesis, and ALB secretion when compared to 2D monolayer culture [176].

Jaksa et al. employed a custom-made 3D printer that can print multiple materials to create a model of a human liver. They used silicone rubber and PDMS oil for the liver model. PLA was used for support structures, which were designed to have specific mechanical and radiological properties. The study had two main objectives. The primary goal was to achieve mechanical realism, while the secondary objective was to achieve radiological similarity. To ensure that printed model resembled native liver in terms of materials, tensile properties, and internal structure were selected. The researchers found that using a liquid-filled internal structure improved the similarity of the model to native liver tissue in terms of both radiological and mechanical aspects compared to bulk silicon and structures without liquid filling. These findings highlight the versatility of extrusion-based multi-material fluid printing as a method for creating functional anatomical models that closely resemble actual tissues, as it successfully replicated both the mechanical and radiological properties of desired tissues [177].

To promote defect liver regeneration, Wang et al. [178] employed droplet microfluidics to generate the photoresponsive cryogel porous microcarrier (CPM) with lipopolysaccharide (LPS) loading immune MSCs activating. When MSC-loaded CPMs were bioprinted in the liver-adapted patches and applied to rats with acute liver failure, they exhibited significantly greater anti-inflammatory and hepatic regenerative properties (Fig. 11a) [178]. To improve hepatic functional restoration, Mao et al. [179] used DLP-based 3D bioprinting to design and engineer novel liver microtissues with internal gear-like structures that achieve greater body surface area (Fig. 11b). Liver dECM was combined with GelMA and encapsulated in human-induced hepatocytes (hiHep cells) to form cell-laden bioink, which exhibited cytocompatibility, printability with excellent mechanical properties (Fig. 11c,d). The incorporation dECM into bioinks enabled hiHep cells to maintain stable viability with sustained liver function metabolism, serving as a potential therapy for partial hepatectomy and chronic liver failure [179].

3.11. Glands

Glandular tissue refers to a type of biological tissue that is specialized for the production and secretion of substances. Glands can be found throughout the body and play various important roles in different physiological processes. Glandular tissue is composed of cells that are specifically designed to produce and secrete substances, such as hormones, enzymes, mucus, sweat, or saliva, depending on the type of gland. These cells are organized into structures that allow for efficient secretion and release of these substances. Exocrine glands and endocrine glands are the two primary categories of glands. Exocrine glands, such as sweat glands or salivary glands, secrete their products onto a body surface or into a cavity through a duct system. Endocrine glands, on the other hand, release their secretions, such as hormones, directly into the blood [180–182]. The technique of gland bioprinting has the potential to create tissue-engineered grafts that can be used for transplantation, potentially replacing or repairing damaged or diseased glands in the future. As a first example, bioprinting has been applied to sweat glands regeneration that plays significant role in thermoregulation. Yuan et al. introduced a novel strategy for directing differentiation of adipose-derived mesenchymal stem cells (ADSCs) to promote regeneration sweat glands by incorporating the specific vascular environment of sweat glands using 3D bioprinting (Fig. 12a). They used sacrificial

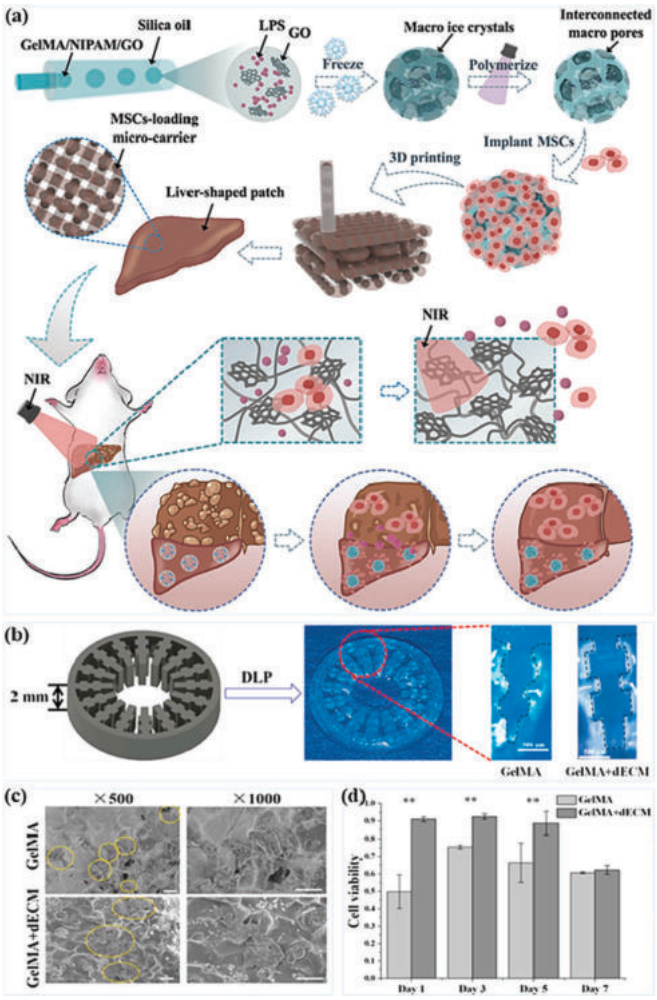

Fig. 11. (a) Schematic representation of manufacturing NIR-responsive CPM & MSC packaging and release; (b) The results of the liver microtissue model, designed and printed using DLP printing; (c) SEM image of cell encapsulation in printed microtissues after a 5d culture; (d) Cell viability in printed microtissues. Reproduced with permission from Refs. [178,179] Copyright 2022 Wiley-VCH & 2020 Elsevier Ltd.

polymer-based templates to generate angiogenic ECM scaffolds, mimicking the physiological interactions between sweat glands and blood vessels *in vitro* (Fig. 12b, c), and facilitated the formation of physiologically relevant angiogenic gland morphology *in vivo* (Fig. 12d, e). Their results confirmed the robustness of the interaction between blood vesels and sweat glands, highlighting the ability of blood vessels to support the regeneration of sweat glands. These findings open up new possibilities for studying the development of sweat glands and the remodeling of blood vessels (Fig. 12f) [183].

Salivary glands have been considered as potential targets for bioprinting to facilitate the spatial organization of cells. Human dental pulp stem cells (hDPSC), which are mesenchymal stem cells derived from the neural crest, were used by Adine et al. in a magnetic 3D bioprinter to produce innervated secretory epithelial organoids without the use of any hydrogels to encapsulate the cells. Following differentiation into salivary gland epithelial cells, cell spheroids were examined in an *ex vivo* transplanted tissue model. Spheroids expressed epithelial compartments of salivary glands, including secretory epithelium, ductal, myoepithelial, and neural. When stimulated with FGF10, the artificial organoids also produced salivary amylase. Additionally, stimulation with different neurotransmitters resulted in the mobilization of intracellular calcium and the induction of *trans*-epithelial resistance [184]. Rodboon et al. developed a practical and detailed procedure for creating lacrimal gland and salivary gland organoids using magnetic 3D bioprinting platforms. This protocol consistently produced organoids that closely resembled the natural parenchymal epithelial tissues of the lacrimal gland or salivary gland [185].

On the other hand, 3D bioprinting of the endocrine gland can be used for studying endocrine gland development, understanding disease mechanisms, and testing new drugs or treatments related to hormone imbalances or deficiencies. As an important endocrine gland, the pancreas is a heterogeneous gland that develops from the posterior foregut of the embryo and emerges as buds from the dorsal and ventral sides of the gut tube. It is composed of two distinct chambers: an endocrine chamber and an exocrine chamber. In human body, pancreas serves two main functions. The exocrine part of the pancreas compose of secretory cells which produce and release digestive enzymes into the pancreatic duct. While endocrine part of pancreas consists of islets that produce hormones and play a role in regulating glucose homeostasis [186]. When pancreas is unable to produce or release sufficient amounts of digestive enzymes or insulin to properly regulate blood sugar levels, the condition is referred to as pancreatic insufficiency which has a significant impact on overall health and digestion [187,188]. A promising treatment option for providing a consistent extrinsic insulin supply is pancreatic islet transplantation. However, after transplantation, there is a significant loss of islet mass and function due to factors such as lack of blood vessels and alloimmune or autoimmune attacks. To address these issues, islets can be protected from the immune system by encapsulating them in a hydrogel matrix, and 3D bioprinting could be used to design favorable hydrogel scaffolds. As a result, this combination of 3D bioprinting and islet encapsulation shows promise in improving the viability and functions of islets [189,190]. Salg et al. manufactured 3D bioprinted building blocks for a hybrid hydrogel and functionalized polycaprolactone scaffold device. After bioprinting, pseudo islet formation from INS to 1 cells produced a viable and proliferative *in vitro* model. Co-culturing these pseudo islets with ECs in a natural cellular niche resulted in improved insulin secretion following glucose stimulation. Additionally, *in vivo* experiments showed that hydrogel and heparinized polycaprolactone both exhibit extensive scaffold vascularization and pseudo-islet survival and function after explantation [191]. In another study, Wang et al. utilized pancreatic ECM (pECM) and hyaluronic acid methacrylate (HAMA) as bioinks to develop a 3D printed islet organoid. To confirm the effectiveness of the HAMA/pECM hydrogel in preserving islet cell morphology and adhesion, they conducted *in vitro* experiments using the Rac1/ROCK/MLCK signaling pathway, which enhances islet function and activity. Moreover, *in vivo* results demonstrated that these 3D printed islet-encapsulated HAMA/pECM hydrogels increased insulin levels in diabetic mice, maintained normal blood glucose levels for 90 days, and promptly released insulin in response to glycemic stimulation. Furthermore, the HAMA/pECM hydrogels were found to promote growth and attachment of new blood vessels, leading to an increase in vessel density [192].

Among other endocrine glands, t he thyroid gland is a relatively simple endocrine organ that produces thyroid hormones. These hormones control the body's metabolic rate, regulate tissue growth and development, and also help regulate blood pressure [193]. Thyroid bioprinting aims to produce tissues that, in terms of structure, cell types, and functionality, closely resemble natural thyroid gland. This has the potential to advance research on thyroid disorders, such as hypothyroidism and hyperthyroidism, as well as provide a means to study thyroid development and test new drugs or treatments. In this context, Bulanova et al. used two typee of rounded embryonic tissue spheroids (thyroid spheroids and allantoic spheroids) on a collagen substrate to bioprint a thyroid gland construct. ECs from allantoic spheroids invaded and vascularized thyroid spheroids, resulting in the formation of a dense capillary network around developing follicles. In a hypothyroid mouse model, the tissue spheroids fused within 4 days to form a single monolithic thyroid construct and restored thyroid activity [194].

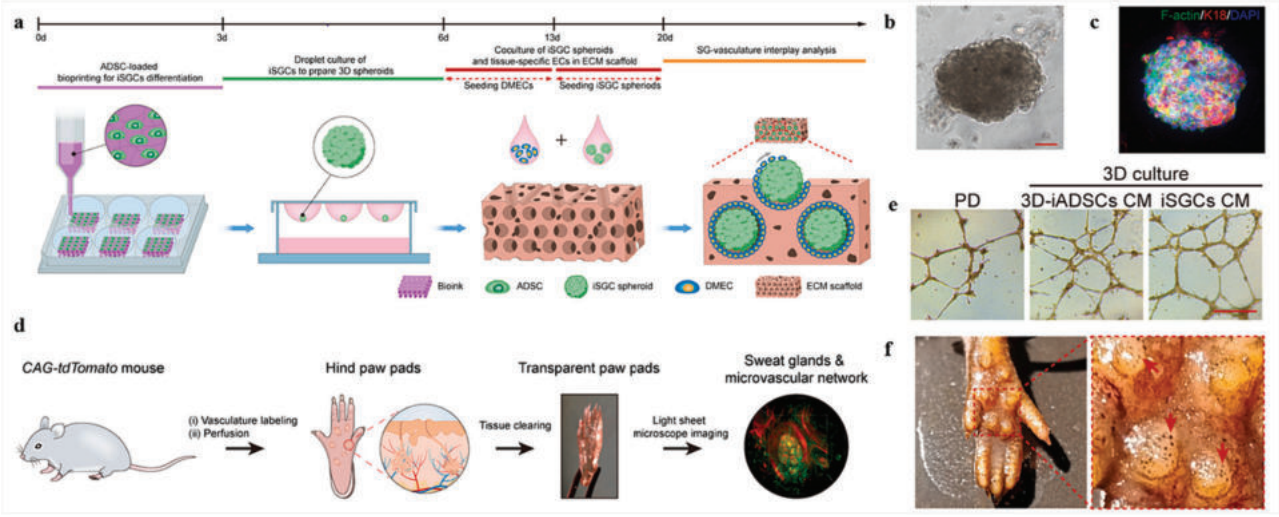

Fig. 12. (a) Schematic illustration of an *in vitro* model that demonstrates the interaction between sweat glands & vasculature, using biomimetic techniques; (b) Formation of induced sweat gland cell spheroids through hanging drop culture; (c) Viability & lineage of induced sweat gland cell spheroids; (d) Schematic demonstration of 3D imaging of the anatomical structure of sweat glands-vasculature using the tissue-clearing technique; (e) Characterization capillary-like structures of dermal microvascular endothelial cells; (f) Sweat assay of mice treated with inducible sweat gland cell spheroids, arrows point to black dots on foot pads (representing activated pores). Reproduced with permission from Ref. [183] Copyright 2023 Elsevier BV.

3.12. Respiratory system

The respiratory system, which includes the lungs, larynx, pharynx, bronchi, trachea, and diaphragm, facilitates the exchange of oxygen and carbon dioxide between the body and the atmosphere. The airway and vasculature are two main parts of lungs. The pulmonary system's primary structural element, the airways, are organized into a branching network. Respiratory diseases and infections are one of the leading causes of death in humans, ranking in the top five. Many chronic lung disorders result in permanent loss of lung function, impaired gas exchange, and reduced quality of life. The only way to treat serious lung diseases in humans due to the human lungs' lack of regeneration capacity is through lung transplantation. The main issues with this procedure, however, are the high cost, the scarcity of donors, and the low success rate. Accordingly, there is a demand for the development of tissue-engineered lungs and lung tissue [195,196].

The use of 3D bioprinting to fabricate lung and tracheal tissue has been accepted as an attractive and reliable method for producing grafts that can be transplanted. In this context, Ng et al. employed the DOD bioprinting technique to successfully fabricate an *in vitro* 3D bioprinted human alveolar lung model. This model consisted of a collagen matrix, alveolar lung epithelium, ECs, and fibroblasts in a high consistency and reproducible manner. The DOD bioprinting technique allowed for precise positioning of various lung cells, resulting in distinct layers in the 3D-printed lung tissue. Additionally, the 3D bioprinted lung tissue models demonstrated excellent viability for at least 14 days. The printed cells remained highly viable and exhibited similar proliferation to non-printed cells [197]. In another study, Rezaei et al. created a new 3D-printed scaffold based on CS/PCL. This scaffold successfully supported and transported the Medical Research Council lung-derived cell line 5 (MRC-5) for pulmonary TE. The combination of CS and PCL can create structures with strong mechanical integrity, comparable to those found in rabbits and rats. Additionally, this combination provides an optimal environment for cell growth, proliferation, and migration within scaffolds [198].

Berg et al. fabricated a humanized 3D bioprinting model for influenza virus infection research. The viability, distribution, and infection efficiency of cells were improved by adjusting the amount of Matrigel in the bioink used for 3D bioprinting of lung models with A549 cells. This optimization resulted in excellent conditions for the bioprinting process. The obtained tissue model confirmed widespread infection by the IAV, with a clustering pattern similar to that observed in the human lung. Furthermore, the printed cells demonstrated a basal immune response by releasing the antiviral IL-29 (interferon λ1) [199]. Besides, 3D bioprinting techniques could serve as a valuable alternative for conducting cytotoxicity studies, especially for lung tissue which is often impacted by viruses like SARS-CoV-2. When conducting toxicity tests, it is important to analyze drugs using a prototype that replicates or mimics the structure and function of the alveoli. Da Rosa et al. successfully created a 3D lung model using sodium alginate and gelatin bioink for drug cytotoxicity testing. They derived the model from human WJ-MSCs that were differentiated into lung cells. The differentiated cells were used to create the 3D lung model *in vitro*. This study was the first to demonstrate the differentiation of MSCs into lung organoids containing four types of lung epithelium [200]. Jung et al. successfully developed two new models for the lower respiratory tract, specifically the alveoli and small airway (Fig. 13a). These models were vascularized and consisted of multiple chips. They used a high throughput, the 64-chip microfluidic plate-based platform for this purpose (Fig. 13b). These models incorporated a microvascular network that could be perfused which was composed of human primary microvascular ECs, pericytes, and fibroblasts. The existing biofabrication protocols also allowed for the formation of distinct layers of lung epithelium at the air–liquid interface (ALI) above vascular tissue layer (Fig. 13c). They co-cultured differentiated alveolar and small airway epithelial cells with pulmonary microvascular ECs, pericytes, and fibroblasts in order to produce a dynamically perfusable microvasculature beneath an ALI-induced epithelial layer (Fig. 13d). Immunostaining on DIV14 confirmed the differentiation of alveolar cells into various subpopulations of ECs (Fig. 13f, e) [201].

cells (including human pulmonary vascular endothelial cells, epithelial cells, fibroblasts, and pericytes); (d) Visual represents the construct of the small alveolar-capillary tissue; (f) Immunofluorescence image of the alveolar layer (Colors represent caveolin-1/CAV1 (cyan), phalloidin (red), DAPI (blue), and ATP-binding cassette class A3/ABCA3 (yellow)). Reproduced with permission from Ref. [201] Copyright 2022 IOP Publishing.

3.13. Urinary system

The urinary system is composed of the kidneys, bladder, ureters, and

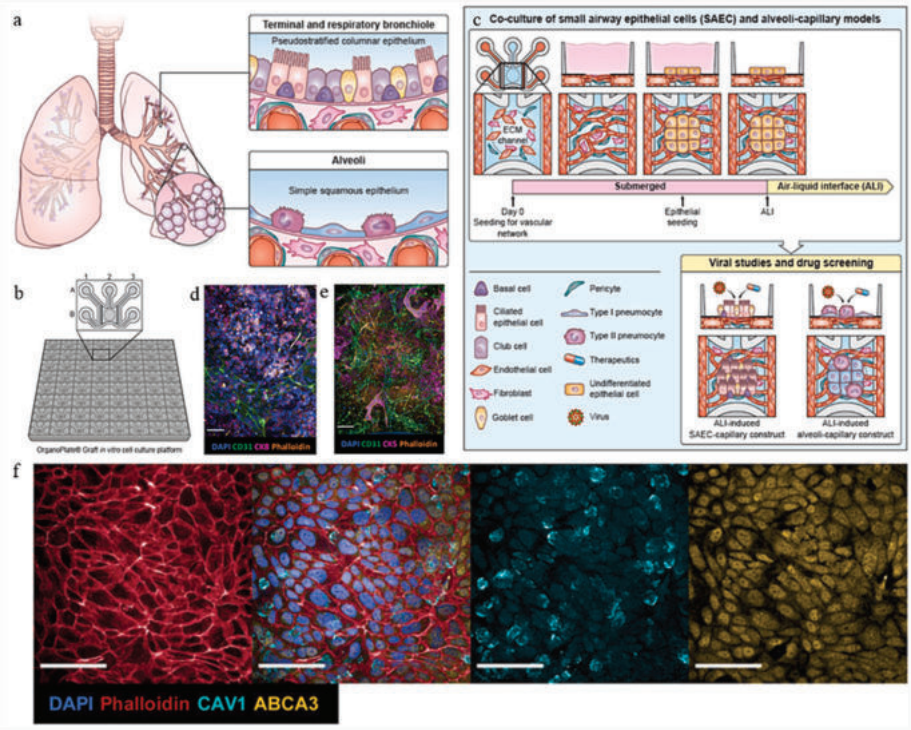

Fig. 13. (a) Schematic representation of human lower respiratory tract's small airways & alveoli; (b) Schematic representation of Mimetas Organograft® 384-well, 64-chip; (c) Timeline depicting the co-culture of vascular cells (including human pulmonary vascular endothelial cells, epithelial cells, fibroblasts, and pericytes); (d) Visual represents the construct of the small alveolar-capillary tissue; (f) Immunofluorescence image of the alveolar layer (Colors represent caveolin-1/CAV1 (cyan), phalloidin (red), DAPI (blue), and ATP-binding cassette class A3/ABCA3 (yellow)). Reproduced with permission from Ref. [201] Copyright 2022 IOP Publishing.

urethra. These organs collaborate to eliminate waste products from the body and maintain fluid and electrolyte balance. All of the other activities attributed to the urinary system are performed by the kidneys, which also produce urine. The urinary bladder serves as a temporary reservoir for the urine and receives the urine from the kidneys after being transported there by the ureters [202]. Urinary system failure occurs when the kidneys are unable to adequately perform their functions, demand renal regenerative therapies such as dialysis, transplantation, and bioprinting. Bioprinting of the urinary system is a promising research field in developing regenerative therapies for the development of regenerative therapies for urinary disorders and kidney diseases [202,203]. Challenges in 3D bioprinting a functional kidney include the complexity of the kidney's architecture, the need for a vascular network to supply nutrients and oxygen to the cells, and the

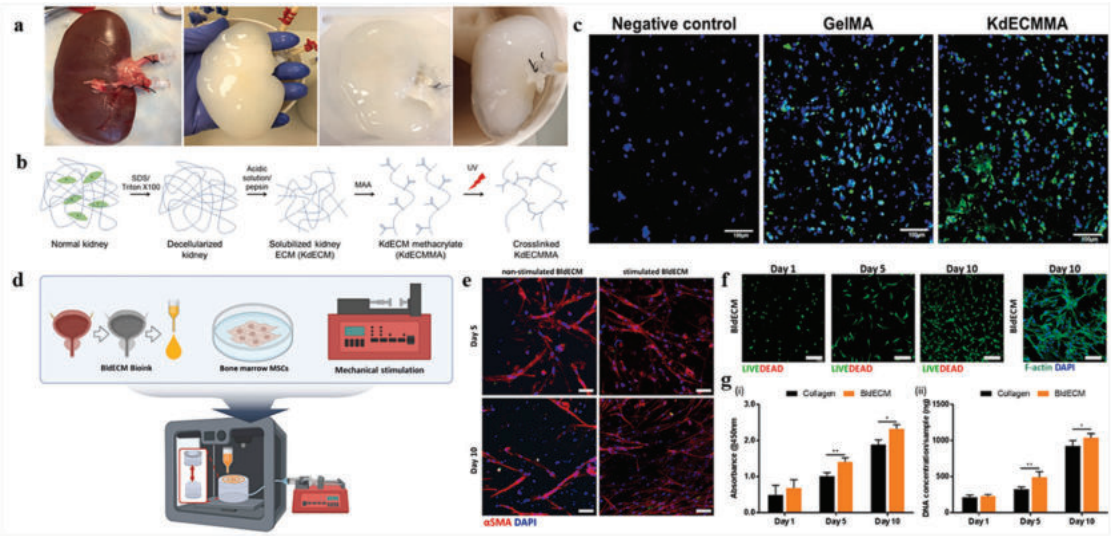

Fig. 14. (a) Process of decellularization of porcine kidney; (b) Schematic representation of photo-crosslinkable ECM hydrogel; (c) The functionality of bioprinted renal structures evaluated *in vitro* through fluorescence image of sodium green expression in bioprinted structures; (d) Schematic illustration of the process of creating an *in vitro* bladder model and tissue-specific bioink, along with a physiological stimulation system; (e) The impact of physiological stimuli on myogenesis in the engineered bladder model; (f) In vitro bio functionality evaluation of hBMSC-loaded BldECM biolink through live/dead & F-actin staining; (g) Cell proliferation in collagen and BldECM compared using: (i) Quantitative CCK-8 and (ii) Quantitative DNA. Reproduced with permission from Refs. [207,213] Copyright 2019 Wiley-VCH, 2022 MDPI.

integration of bioprinted tissue with recipient's body. Additionally, ensuring the functionality and longevity of the bioprinted kidney tissue is a critical aspect of successful transplantation. However, considerable advancements have been made in the laboratory bioprinting of kidney tissue [204–206]. For example, Ali et al. developed a photo-crosslinkable bioink derived from kidney ECM, in order to establish a kidney-specific microenvironment. This bioink was designed to facilitate the maturation of human kidney cells and the formation of renal tissue. The outcomes demonstrated that the KdECMMA bioink-printed human kidney cells were extremely viable and matured over time (Fig. 14a, b). Thus, high cell viability and proliferation as well as the structural and functional characteristics of the native renal tissue were all visible in the bioprinted renal tissue constructs (Fig. 14c) [207]. To fabricate localized patterns of renal epithelial cells embedded in a hydrogel matrix, Xu et al. employed drop-on-demand bioprinting. Bioprinting allowed for the control of self-assembly processes, resulting in perfusable, size-defined, scalable, and oriented epithelial cell spheroids and nephron-like tubules with a lumen. This achievement was crucial for advancing 3D nephron models in screening applications, particularly in nephrotoxicity studies, where the ability to scale fabrication processes remains a restricting factor [208].

The kidney exhibits a hierarchical organization, encompassing both the macro-level, which entails prominent components like renal arteries, veins, and ureters, and the micro-level, which involves intricate structures such as nephrons - approximately one million intricate functional units - and the stroma occupying the interstitial space between nephrons [209]. Accurately replicating these complex structures at the micro-level poses a significant challenge. Firstly, the selection of renal cell types is a formidable task due to the existence of over 20 distinct cell types, including glomerular podocytes, proximal and distal tubular epithelial cells, mesangial cells, and endothelial cells, among others. Precisely determining the appropriate positioning of these cell types is an immensely challenging endeavor. Moreover, the identification of suitable biomaterials that facilitate the preservation of kidney structure and function after 3D bioprinting is a complex undertaking. These challenges collectively impede the straightforward generation of transplantable kidneys using individual technologies. However, they can serve as valuable platforms for investigating renal diseases and conducting drug screening experiments [210]. A study reported extrusion-based bioprinting to deposit nephron progenitors derived from induced pluripotent stem cells (iPSCs). Subsequently, conventional culture at the air–liquid interface was employed to induce the differentiation of these progenitors into nephrons. Instead of printing multiple differentiated cell types, the study focused on manually differentiating the nephron progenitors, thereby facilitating the generation of conventional nephron organoids. Although the ratios of glomeruli and renal tubules in these manually-generated organoids exhibited some variations, the extrusion-based bioprinting technique enabled the rapid and high-throughput production of kidney organoids with consistent cell numbers and ratios of cell types. Furthermore, flattening the organoids resulted in enhanced maturity and increased nephron count, likely due to improved oxygen and nutrient accessibility throughout the organoids owing to their uniform and reduced tissue height [211]. If 3D bioprinting technology can be harnessed to precisely control the positioning of not only nephron progenitors but also other types of progenitors, the resulting aggregates may consistently form higher-order structures and potentially contribute to the development of transplantable kidneys [210].

Bioprinting technology has also enabled the development of artificial bladders to treat bladder injuries. In this regard, Zhang et al. fabricated a synthetic urethra that mimicked the natural urethra of rabbits by using integrated bioprinting technology. The urethra was fabricated from thermoplastic polymers of PCL and poly(lactide-co-caprolactone) (PLCL), along with fibrin, hyaluronic acid, and gelatin bioink containing smooth muscle cells (SMCs) and urethral epithelial cells (UCs). After 7 days, cells viability remained above 80 %, and the printed structure possessed similar morphological and mechanical properties to the native urethra of rabbits. The specific biomarkers were still present in cell-laden hydrogel and both cell types demonstrated active proliferation [212]. In a proof-of-concept study by Chae et al., a platform of bladder-mimicking with a mechanical stimulation system was developed as an *in vitro* model of the urinary bladder. This biomimetic model system, developed using 3D bioprinting, was able to mimic the natural movement of the urinary bladder by incorporating bladder tissue derived from dECM and utilizing cyclic mechanical stimuli (Fig. 14d), was able to mimic the natural movement of the urinary bladder. The findings demonstrated that when exposed to dynamic mechanical cues, developed bladder tissue models showed potential for myogenic differentiation (Fig. 14e) potential and displayed high cell viability and proliferation rates (Fig. 14f, g) [213].

3.14. Reproductive system

The reproductive system is a complex system of the human body responsible for producing offspring. It includes organs, glands, and hormones that work together to enable sexual reproduction. The survival of the species relies on the reproductive system. Both males and females can become infertile for a variety of reasons. Patients undergoing treatment for cancer and and autoimmune diseases often experience impaired ovarian function, which can lead to loss of puberty, infertility, and premature menopause [214,215]. Current methods of artificial reproduction and hormone restoration, such as ovary transplants and assisted fertilization, are not long-term solutions and could result in metastatic diseases for pediatric patients. Moreover, the limited availability of autologous tissue for reconstructive surgery presents a significant obstacle in treating genital abnormalities. TE and bioprinting offer alternative treatment techniques to overcome this limitation. However, bioprinting of the entire reproductive system remains a complex and challenging endeavor [31,216–218]. The development of engineered ovarian tissues is particularly promising in the field of TE, as ovarian deficiency is the most common cause of female infertility [218].

As a first attempt to reach this goal, Laronda et al. used 3D-printed human ovarian tissues and acellular bovine to promote follicle growth and restore ovarian function that had undergone ovariectomies. They demonstrated that follicular viability and function were greatly affected by the pore geometry of gelatin scaffolds, with 30° and 60° providing corners that surround the follicle on multiple sides and facilitate the interaction between scaffolds and follicles. When the follicle-seeded 3D scaffolds were implanted in sterilized mice, they developed into highly vascularized structures. As a result, the mice's ovarian function was completely restored. Most notably, they successfully achieved natural mating and born mouse pups as a result [219]. Zheng et al. fabricated 3D porous cylindrical ovarian structures using swine ovary dECM-based bioink to encapsulate primary ovarian cells (POC) to correct ovarian insufficiency in mice. To test the effectiveness of the 3D scaffolds, a female castrated mouse model was used. The findings demonstrated that the group treated with the 3D scaffold containing POCs exhibited more favorable indicators of neoangiogenesis, cell proliferation, and cell survival compared to the group treated with only the 3D scaffold. Additionally, this group also ensures the secretion of sex hormones [220]. In another study, Wu et al. used exogenous follicles deposited in the scaffolds to create a 3D bioprinted ovary using GelMA bioink. The GelMA-based scaffolds demonstrated excellent shape fidelity and hygroscopicity. The researchers utilized commercially available ovarian tumor cell lines and primary ovarian somatic cells for the 3D printing process involving cells. However, the viability of the primary ovarian cells was lower compared to the commercial cell lines. Therefore, it was not suitable to create 3D structures from primary ovarian cells using an extrusion-based technique. Nevertheless, the ovarian follicles successfully expanded and ovulated within the scaffolds, thanks to the GelMA-based 3D printing system providing the appropriate microenvironment. Furthermore, after *in vitro* maturation, metaphase II oocytes were observed [221].

Bioprinting the uterus is a complex and challenging due to the intricate structure and functions of this organ. While there have been advancements in the field of bioprinting, 3D bioprinting fully functional uterus is still in the early stages of research [222,223]. However, scientists have started exploring this possibility and have made some progress. For instance, Souza et al. successfully developed an *in vitro* 3D model of human myometrial cells to study different pathological conditions that affect maternal health. They used magnetic bioprinting to fabricate hollow rings resembling cross-sections of the uterus. The patients exhibited varying contractile patterns and responded differently to the clinically relevant tocolytic agents, nifedipinei and indomethacin. This system not only allowed for high-throughput testing of different agents and conditions but also served as an effective tool for assessing the physiology of human parturition [224]. To restore the structure and fertility of damaged uterine endometrium, Nie et al used 3D extrusion-based bioprinting. They created a bilayer endometrial construct (EC) using a hydrogel made of sodium alginate and hyaluronic acid (Alg-HA) designed to regenerate the endometrium and improve its function (Fig. 15a). The upper layer of the EC consisted of a single layer of endometrial epithelial cells (EECs), while the lower layer had a grid-like microstructure filled with endometrial stromal cells (ESCs) (Fig. 15b). In an animal model of uterine injury, the 3D bio-printed EC was applied to restore the endometrial structure and improve pregnancy outcomes (Fig. 15c). The repair of the severely damaged endometrium, including the regeneration of the endometrium, glands, and other tissues, was indicative of the therapeutic effect of the 3D bio-printed bilayer EC. Additionally, bioprinted ECs ameliorated fertility decline in the injured uterus (Fig. 15d, e) [225]. *In vivo* bioprinting enables the creation of 3D structures directly inside living animals to repair or reconstruct tissues. However, there are challenges in using this technique in the confined subaqueous space of fetal membranes (FMs). Zhao et al. proposed a new method called subaqueous *in vivo* bioprinting, which involves using a 7-axis robot-assisted minimally invasive approach. This approach aims to address the issue of premature rupture of membranes (PROM), which is the breakage of the amniotic sac before delivery. Hydrogel patches were printed subaqueously using specially designed gel rivets. These patches have mechanical properties similar to native tissue, strong tissue adhesion, good biocompatibility, and can effectively seal the rupture to prolong pregnancy. The sealing effect for PROM observed in mid-gestational rabbit models and *in vitro* uterus models supported the applicability of their subaqueous bioprinting method [226].

While most TE studies focused on female reproductive organs, research on bioprinting cells or tissue related to the male reproductive system is limited and needs further exploration. Recently, Robinson et al. conducted a study to investigate the possibility and potential of using 3D bioprinting to create personalized human testicular cells from a patient with nonobstructive azoospermia (NOA). Their study demonstrated for the first time that adult human testicular cells could be successfully 3D bioprinted. They found that the bioprinting procedure preserved a high level of testicular cell viability and did not lead to the primary somatic phenotypes to disappear from the testis tissue. Furthermore, after 12 days of *in vitro* culture, they also noticed a rise in germ cell markers inside the 3D bioprinted tubules [227]. In another study, Bashiri et al. conducted research on the process of spermatogenesis using a printing structure derived from the ECM of testicular tissue (T-ECM). The researchers decellularized ram testis tissue using a

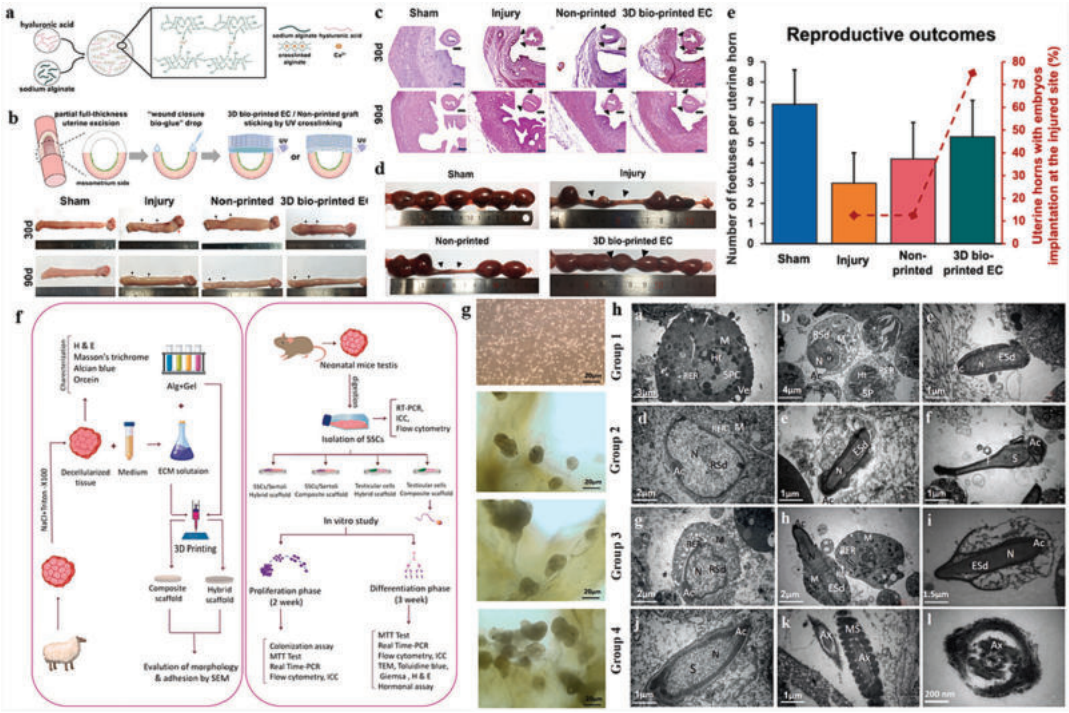

Fig. 15. (a) Schematic representation of crosslinking process of Alg-HA hydrogels; (b) Schematic representation of the partial & full-thickness removal of the uterus, followed by the implantation of 3D biologically printed EC or non-printed grafts. The regenerated endometrium was analyzed morphologically & histologically in different treatment groups (In the injury group, effusion is indicated by a red triangle, while the surgical site is indicated by a black triangle); (c) H&E staining to examine each group's histological structure; (d) Pregnancy outcome of the different groups 90 days after surgery; (e) Evaluation of reproductive results following uterine regeneration in different groups; (f) Extraction of ECM from ram testis & bioengineering of 3D printed scaffolds as well as proliferation and differentiation of mouse SSCs on 3D printed scaffolds; (g) Evaluation of cell morphology during proliferation; (h) Ultrastructure analysis of cells cultured on a 3D printed system following the differentiation stage (In group 1 (a–c), round and elongating spermatids with distinct nuclei, Golgi vesicles and mitochondria were observed, along with secondary spermatocytes. In group 2 (d–f), similar cells to elongated spermatids were found, with round and elongated spermatids displaying distinct small heads, necks, and tails. The morphology of spermatids during the development of the cap and acrosome stage is shown in group 3 (g–i). In Group 4 (j–l), the head exhibited nucleus and acrosome structures, while the tail showed an axoneme structure, dense external fibers, mitochondrial helix, a longitudinal column of the fibrous sheath, and a plasma membrane surrounding the cell). Reproduced with permission from Refs. [225,228] Copyright 2022, 2023 Elsevier BV.

hypertonic solution containing Triton. They then used the extracted ECM as a bioink to print artificial testes (Fig. 15f). The 3D-printed scaffolds derived from T-ECM had small pore sizes, which allowed for the release of growth factors necessary for cell growth. These scaffolds also promoted the formation of cell junctions, enhancing the viability and proliferation of spermatogonial stem cells (SSCs) which resulted in improved nutrient availability and gas exchange (Fig. 15g). When neonatal mouse testicular cells were cultured on T-ECM scaffolds, they developed into morphologically mature spermatozoa in a short period. Additionally, the scaffolds supported the ability of the testicular cells to secrete inhibin B and testosterone (Fig. 15h) [228].

4. Challenges and limitations

3D bioprinting has great potential to revolutionize TE and regeneration and and plays an important role in personalized medicine by enabling the design, prototyping, and fabrication of 3D tissue structures for various therapies. It seems that, as studies progress, in situ/*in vivo* bioprinting is moving forward in popularity [260]. Although 3D bioprinting has progressed considerably, the entire biofabrication platform needs to be standardized and integrated, from software design to processing tissues after printing. To develop next-generation bioengineered tissues, it is essential to address the drawbacks of biofabrication platforms in terms of speed, complexity, material selection, printing resolution, and cell processing. There are unique challenges associated with using 3D bioprinting technology. In order to enable its widespread adoption, several challenges in the tissue maturation steps in pre-printing, printing, and post-printing need to be addressed [261]. Specifically, the choice of bioink is one of the most important aspects of bioprinting which helps to circumvent some of these challenges. Bioinks are used to mimic the complex structure and composition of different organs and tissues. They act as a medium to protect cells during the printing process and provide a suitable environment for the development of micro-tissues to mature following printing. Selecting the approprite bioinks is crucial as they provide the necessary chemical and physical signals for cells to interact with the ECM, as the properties of the bioink affect the cell growth and proliferation, as well as cell structure and function. Typically, natural or synthetic polymers, alone or combined together, are developed as bioinks that can impart structural integrity and mechanical properties to tissues and mimic their biochemical environment [261,262]. Meanwhile, some materials serve as sacrificial supporting materials which hold the cells together during printing and are removed immediately after printing [263].

On the other hand, to achieve the desired fabricated tissue equivalent important bioink properties such as rheological characteristics, cell–ECM interactions, gelation kinetics, material properties, and cell source should be considered [261]. It is important that the bioink formulation be stable enough to ensure that the tissue construct remains structurally stable. Hence, the bioprinted hydrogel matrix must be controlled in terms of its rheological and geometrical properties as well as stiffness to result in optimal tissue development and maturation [264]. Bioink should have a viscosity that is suitable for both cell growth and differentiation, as well as printing; however, practically, suitable viscosity for bioprinting may not support cell viability. Additionally, the printability of bioinks, i.e. the ease of printing at a proper resolution, and the ability to preserve the structure are influenced by the specific type of bioprinting technique used, and this process can affect cell viability. Therefore, it is crucial to optimize the printing conditions and bioink consistency in order to strike a balance between bioink printability and cell viability. Shear stress, on the other hand, can affect cell viability and bioink stability [265]. If composite bioinks comprising hard inclusions are used, such as polymer-based inks for bone applications in which calcium phosphate ar bioactive glass particles are dispersed due to their ability to stimulate mineralization and osteogenesis, additional challenges should be considered. The size and shape of bioceramic particles in the ink should be carefully selected to avoid damage to cells and to properly modulate the viscosity.

Besides all these considerations, bioinks should be biocompatible and support cells to facilitate functional cell differentiation into target tissues; moreover, bioinks should be biodegradable to prevent any long-term reactions [266]. Another consideration is cellular sources for constructing 3D bioprinted tissues. Primary cells are mostly pre-harvested *in vitro* before heterogeneous tissue constructs are bioprinted. To avoid an immune reaction, primary cells for transplantation are removed from the patient. Moreover, cell behavior of the constructed structures determines the function of the constructs [8,267].

On the other hand, the success of tissue regeneration depends on cell viability, which can be greatly impacted by bioprinting techniques. Shear stress, pressure, temperature, exposure duration, and the characteristics of the bioink are variables that affect cell viability in different bioprinting techniques [39]. For example, in extrusion-based bioprinting shear stress and pressure applied during extrusion may have an impact on the viability of cells. High levels of shear stress or pressure can damage cells, resulting in reduced viability [56]. Inkjet-based bioprinting may subject cells to mechanical and thermal stresses during the droplet formation process, potentially compromising the cell viability [268]. However, it is important to note that while thermal and shear stress can denature hydrogel materials and affect cell viability, the processing time in this technique is very short, which helps to maintain the stability of biomaterials and the functionality and proliferation capacity of cells [39]. Laser-assisted bioprinting provides precise control over the formation and deposition of droplets, minimizing the impact on cell viability. Moreover, the contact time between cells and the laser is typically brief, reducing the risk of thermal damage [269]. Moreover, droplet-based bioprinting allows for high cell viability by reducing exposure to shear stress. The gentle and precise deposition of droplets minimizes cell damage, leading to improved cell viability [270]. By optimizing printing parameters such as nozzle size, extrusion pressure, and bioink properties, it is possible to minimize these negative effects and enhance cell viability [39].

Processing time and cost are the other major challenges that prevent mass production and should be analyzed in each specific application. Nonetheless, bioprinting can be more cost-effective for customized products with complex and hierarchical structures [271]. Another challenge that should be mentioned is scalability and the concurrent changes associated with upscaling. It is entirely possible that the molecular properties of bioink contradict the morphology of large animals [272]. Aside from these technical challenges, there are several ethical concerns regarding the potential implications of 3D bioprinting for humans [273].

5. Conclusions and future perspective

Bioprinting is an innovative and advanced fabrication technique that could develop rapid-prototyped 3D tissue constructs from cell-laden hydrogels, mimicking the intricacies of natural tissues and networks. This revolutionary technology offers customized production with the freedom to design complex and heterogeneous tissue structures and the ability to precisely dispense bioink with a high spatial and temporal resolution with minimum waste for niche applications. In addition, developing new dynamic post-printing tissue maturation systems and reducing mechanical and rheological shortcomings of bioinks, as well as improving printing speed and accuracy will further facilitate this technology to be widely adopted and used [261,274,275]. Besides, the simplicity, flexibility, and versatility of this technique, compared with conventional techniques, allow for the construction of a highly controlled internal microenvironment with controlled spatial cell distribution, which ultimately facilitates cell behaviors including growth, proliferation, differentiation, etc. Therefore, significant development of 3D bioprinting has provided prominent opportunities in terms of understanding organ systems and transplantable tissue production in healthcare and therapeutic use. However, various challenges such as the

complete understanding of the level of biomimetic complexity of native organs or tissues required to perform relevant tissue and organ replacements and achieve functional recovery, as well as the differentiation of PSCs into the required phenotypes, remain to be fully solved when approaching complex tissue regeneration strategies, thus limiting the ultimate exploitation of the true potential of various bioprinting technologies [276,277].

With advances in technological processes, computational modeling, artificial intelligence, and machine learning, as well as more comprehensive understanding of the optimal interactions between biomaterials and cells will significantly improve the biomimetic capabilities of bioprinted tissues in the coming years. In this direction, bioprinting can be applied to create complex and biomimetic tissues, allowing for the inclusion of vascular, lymphatic, and neural networks. This approach captures the intricate nature of various tissues and organ systems at a cellular scale resolution. Although the progression of in-situ bioprinting by using robotic arms and handheld devices could be utilized to fabricate anisotropic biological tissue and its growth pattern represents a promising pathway to address existing defects, integrating multidisciplinary innovations is required for the development of simultaneous and/or sequential operation of patient monitoring, medical imaging, multiaxial feedback control systems, and feedback control for future clinical translation of this technology. Advanced bioinformatics tools such as artificial intelligence, along with a thorough understanding of the various fields involved, can enable computers to have similar learning capacity as humans. The powerful capability to process large data sets and detect deep relationships and features within the data allows navigating the vast amount of data generated by bioprinting, thus obtaining more accurate models by identifying patterns and making predictions from the data with minimal human intervention. Furthermore, detecting defects, optimizing processes, and analyzing dimensional accuracy in 3D bioprinting will be possible and practicable to streamline manufacturing processes in the future.

CRediT authorship contribution statement

Mojdeh Mirshafiei: Conceptualization, Investigation, Methodology, Writing – original draft. **Hamid Rashedi:** Conceptualization, Investigation, Methodology, Writing – original draft. **Fatemeh Yazdian:** Conceptualization, Investigation, Methodology, Supervision, Writing – original draft. **Abbas Rahdar:** Conceptualization, Investigation, Methodology, Writing – review & editing. **Francesco Baino:** Conceptualization, Investigation, Methodology, Validation, Writing – review & editing.

Declaration of competing interest

The authors declare that they have no known competing financial interests or personal relationships that could have appeared to influence the work reported in this paper.

Data availability

Data will be made available on request.

Acknowledgment

Abbas Rahdar thanks from University of Zabol for funding (UOZ-GR-8906).

References

[1] R. Burdis, D.J. Kelly, Biofabrication and bioprinting using cellular aggregates, microtissues and organoids for the engineering of musculoskeletal tissues, Acta Biomater. 126 (2021) 1–14.
[2] A.-F.-J. de Kanter, et al., The ethical implications of tissue engineering for regenerative purposes: a systematic review, Tissue Eng. B Rev. 29 (2) (2023) 167–187.
[3] V. Mishra, S. Negi, S. Kar, FDM-based additive manufacturing of recycled thermoplastics and associated composites, J. Mater. Cycles Waste Manage. 25 (2) (2023) 758–784.
[4] X. Zhang, et al., Additive manufacturing of cellular ceramic structures: From structure to structure–function integration, Mater. Des. 215 (2022) 110470.
[5] Q. Zhang, et al., Shedding light on 3D printing: Printing photo-crosslinkable constructs for tissue engineering, Biomaterials 286 (2022) 121566.
[6] D. Akilbekova, A. Turlybekuly, Patient-specific 3D bioprinting for in situ tissue engineering and regenerative medicine, in: 3D Printing in Medicine, Elsevier, 2023, pp. 149–178.
[7] G. Größbacher, et al., Volumetric printing across melt electrowritten scaffolds fabricates multi-material living constructs with tunable architecture and mechanics, Adv. Mater. (2023) 2300756.
[8] J.M. Lee, W.Y. Yeong, Design and printing strategies in 3D bioprinting of cell-hydrogels: A review, Adv. Healthc. Mater. 5 (22) (2016) 2856–2865.
[9] C.K. Chua, K.F. Leong, C.S. Lim, Rapid prototyping: principles and applications (with companion CD-ROM), World Scientific Publishing Company, 2010.
[10] D. Trucco, et al., Modeling and fabrication of silk fibroin–gelatin-based constructs using extrusion-based three-dimensional bioprinting, ACS Biomater Sci. Eng. 7 (7) (2021) 3306–3320.
[11] A. Lee, et al., 3D bioprinting of collagen to rebuild components of the human heart, Science 365 (6452) (2019) 482–487.
[12] D.G. Nguyen, et al., Bioprinted 3D primary liver tissues allow assessment of organ-level response to clinical drug induced toxicity in vitro, PLoS One 11 (7) (2016) e0158674.
[13] A.M. Hughes, et al., Printing the pathway forward in bone metastatic cancer research: applications of 3D engineered models and bioprinted scaffolds to recapitulate the Bone-Tumor Niche, Cancers 13 (3) (2021) 507.
[14] A. McMillan, et al., 3D bioprinting in otolaryngology: A review, Adv. Healthc. Mater. (2023) 2203268.
[15] Y. Xu, et al., A multifunctional 3D bioprinting system for construction of complex tissue structure scaffolds: design and application, Int. J. Bioprinting 8 (4) (2022).
[16] S. Vijayavenkataraman, et al., 3D bioprinting of tissues and organs for regenerative medicine, Adv. Drug Deliv. Rev. 132 (2018) 296–332.
[17] W. Dai, et al., 3D bioprinting of heterogeneous constructs providing tissue-specific microenvironment based on host–guest modulated dynamic hydrogel bioink for osteochondral regeneration, Adv. Funct. Mater. 32 (23) (2022) 2200710.
[18] S. Panda, et al., A focused review on three-dimensional bioprinting technology for artificial organ fabrication, Biomater. Sci. 10 (18) (2022) 5054–5080.
[19] F.-M. Chen, X. Liu, Advancing biomaterials of human origin for tissue engineering, Prog. Polym. Sci. 53 (2016) 86–168.
[20] S.J. Lee, J.J. Yoo, A. Atala, Biomaterials and tissue engineering, Clin. Regen. Med. Urol. (2018) 17–51.
[21] A. Bakhtiiari, et al., A bioprinted composite hydrogel with controlled shear stress on cells, Proc. Inst. Mech. Eng. [H] 235 (3) (2021) 314–322.
[22] J. Malda, et al., 25th anniversary article: engineering hydrogels for biofabrication, Adv. Mater. 25 (36) (2013) 5011–5028.
[23] H. Zhu, et al., 3D bioprinting of multifunctional dynamic nanocomposite bioinks incorporating Cu-doped mesoporous bioactive glass nanoparticles for bone tissue engineering, Small 18 (12) (2022) 2104996.
[24] H. Amani, et al., Controlling cell behavior through the design of biomaterial surfaces: a focus on surface modification techniques, Adv. Mater. Interfaces 6 (13) (2019) 1900572.
[25] S. Pradhan, et al., Biofabrication strategies and engineered in vitro systems for vascular mechanobiology, Adv. Healthc. Mater. 9 (8) (2020) 1901255.
[26] A. Schwab, et al., Printability and shape fidelity of bioinks in 3D bioprinting, Chem. Rev. 120 (19) (2020) 11028–11055.
[27] S. Derakhshanfar, et al., 3D bioprinting for biomedical devices and tissue engineering: A review of recent trends and advances, Bioact. Mater. 3 (2) (2018) 144–156.
[28] M.E. Prendergast, J.A. Burdick, Recent advances in enabling technologies in 3D printing for precision medicine, Adv. Mater. 32 (13) (2020) 1902516.
[29] N. Wang, et al., A review of multi-functional ceramic nanoparticles in 3D printed bone tissue engineering, Bioprinting 23 (2021) e00146.
[30] W. Sun, et al., The bioprinting roadmap, Biofabrication 12 (2) (2020) 022002.
[31] C. Mota, et al., Bioprinting: from tissue and organ development to in vitro models, Chem. Rev. 120 (19) (2020) 10547–10607.
[32] A. Sarkar, et al., hemical synthesis of silk-mimetic polymers, Materials 12 (24) (2019) 4086.
[33] J. Groll, et al., Biofabrication: reappraising the definition of an evolving field, Biofabrication 8 (1) (2016) 013001.
[34] S. Singh, et al., In situ bioprinting–bioprinting from benchside to bedside? Acta Biomater. 101 (2020) 14–25.
[35] B. Yilmaz, A. Tahmasebifar, E.T. Baran, Bioprinting technologies in tissue engineering, in: Current Applications of Pharmaceutical Biotechnology, Springer, 2019, pp. 279–319.
[36] X. Li, et al., Inkjet bioprinting of biomaterials, Chem. Rev. 120 (19) (2020) 10793–10833.
[37] Q. Wei, et al., Modification, 3D printing process and application of sodium alginate based hydrogels in soft tissue engineering: A review, Int. J. Biol. Macromol. (2023) 123450.

[38] Z. Wang, et al., 3D bioprinting of emulating homeostasis regulation for regenerative medicine applications, J. Controll. Release 353 (2023) 147–165.
[39] J. Adhikari, et al., Effects of processing parameters of 3D bioprinting on the cellular activity of bioinks, Macromol. Biosci. 21 (1) (2021) 2000179.
[40] H.-G. Yi, et al., Application of 3D bioprinting in the prevention and the therapy for human diseases, Signal Transduct. Target. Ther. 6 (1) (2021) 177.
[41] H. Ebrahimi Orimi, et al., Drop-on-demand cell bioprinting via Laser Induced Side Transfer (LIST), Sci. Rep. 10 (1) (2020) 9730.
[42] W. Li, et al., Stereolithography apparatus and digital light processing-based 3D bioprinting for tissue fabrication, Iscience, 2023.
[43] C.A. Murphy, K.S. Lim, T.B. Woodfield, Next evolution in organ-scale biofabrication: bioresin design for rapid high-resolution vat polymerization, Adv. Mater. 34 (20) (2022) 2107759.
[44] A. Madrid-Sánchez, et al., Fabrication of large-scale scaffolds with microscale features using light sheet stereolithography, Int. J. Bioprinting 9 (2) (2023).
[45] C. Greant, et al., Digital light processing of poly (ε-caprolactone)-based resins into porous shape memory scaffolds, Eur. Polym. J. (2023) 112225.
[46] H.W. Ooi, et al., Thiol–ene alginate hydrogels as versatile bioinks for bioprinting, Biomacromolecules 19 (8) (2018) 3390–3400.
[47] S. Michael, et al., Tissue engineered skin substitutes created by laser-assisted bioprinting form skin-like structures in the dorsal skin fold chamber in mice, PLoS One 8 (3) (2013) e57741.
[48] X. Jing, et al., Two-photon polymerization for 3D biomedical scaffolds: Overview and updates, Front. Bioeng. Biotechnol. 10 (2022) 994355.
[49] L.K. Shopperly, et al., Blends of gelatin and hyaluronic acid stratified by stereolithographic bioprinting approximate cartilaginous matrix gradients, J. Biomed. Mater. Res. B Appl. Biomater. 110 (10) (2022) 2310–2322.
[50] J. Zhang, et al., Single cell bioprinting with ultrashort laser pulses, Adv. Funct. Mater. 31 (19) (2021) 2100066.
[51] Y. Xiang, et al., 3D bioprinting of complex tissues in vitro: State-of-the-art and future perspectives, Arch. Toxicol. 96 (3) (2022) 691–710.
[52] A. Enrico, et al., 3D microvascularized tissue models by laser-based cavitation molding of collagen, Adv. Mater. 34 (11) (2022) 2109823.
[53] A. Zennifer, A. Subramanian, S. Sethuraman, Design considerations of bioinks for laser bioprinting technique towards tissue regenerative applications, Bioprinting 27 (2022) e00205.
[54] P. Maturavongsadit, et al., Cell-laden nanocellulose/chitosan-based bioinks for 3D bioprinting and enhanced osteogenic cell differentiation, ACS Appl. Biol. Mater. 4 (3) (2021) 2342–2353.
[55] F. Züger, N. Berner, M.R. Gullo, Towards a novel cost-effective and versatile bioink for 3D-bioprinting in tissue engineering, Biomimetics 8 (1) (2023) 27.
[56] S. Boularaoui, et al., An overview of extrusion-based bioprinting with a focus on induced shear stress and its effect on cell viability, Bioprinting 20 (2020) e00093.
[57] J. Karvinen, M. Kellomäki, Design aspects and characterization of hydrogel-based bioinks for extrusion-based bioprinting, Bioprinting (2023) e00274.
[58] N.M. Pu'ad, et al., Review on the fabrication of fused deposition modelling (FDM) composite filament for biomedical applications, Mater. Today:. Proc. 29 (2020) 228–232.
[59] H. Zhang, C. Wu, 3D printing of biomaterials for vascularized and innervated tissue regeneration, Int. J. Bioprinting 9 (3) (2023).
[60] R. Li, et al., Decorating 3D printed scaffolds with electrospun nanofiber segments for tissue engineering, Adv. Biosyst. 3 (12) (2019) 1900137.
[61] H. Jeon, C.G. Simon Jr, G. Kim, A mini-review: cell response to microscale, nanoscale, and hierarchical patterning of surface structure, J. Biomed. Mater. Res. B Appl. Biomater. 102 (7) (2014) 1580–1594.
[62] I. Maliszewska, T. Czapka, Electrospun polymer nanofibers with antimicrobial activity, Polymers 14 (9) (2022) 1661.
[63] D.L. Yang, et al., Combination of 3D printing and electrospinning techniques for biofabrication, Adv. Mater. Technol. 7 (7) (2022) 2101309.
[64] C. Richard, A. Neild, V.J. Cadarso, The emerging role of microfluidics in multi-material 3D bioprinting, Lab Chip 20 (12) (2020) 2044–2056.
[65] A.K. Miri, et al., Multiscale bioprinting of vascularized models, Biomaterials 198 (2019) 204–216.
[66] E. Davoodi, et al., Extrusion and microfluidic-based bioprinting to fabricate biomimetic tissues and organs, Adv. Mater. Technol. 5 (8) (2020) 1901044.
[67] A. Chen, et al., Multimaterial 3D and 4D Bioprinting of heterogenous constructs for tissue engineering, Adv. Mater. (2023) 2307686.
[68] B. Zhang, et al., Electrohydrodynamic printing of submicron-microscale hybrid scaffolds with improved cellular adhesion and proliferation behaviors, Nanotechnology 34 (10) (2022) 105102.
[69] K. Patel, H. Stark, Fluid interfaces laden by force dipoles: towards active matter-driven microfluidic flows, Soft Matter 19 (12) (2023) 2241–2253.
[70] L. Zhao, X. Wang, 3D printed microfluidics for cell biological applications, TrAC Trends Anal. Chem. 158 (2023) 116864.
[71] A.S. Mao, D.J. Mooney, Regenerative medicine: current therapies and future directions, Proc. Natl. Acad. Sci. 112 (47) (2015) 14452–14459.
[72] D. Yoo, New paradigms in hierarchical porous scaffold design for tissue engineering, Mater. Sci. Eng. C 33 (3) (2013) 1759–1772.
[73] S. Zhang, et al., A review on the use of computational methods to characterize, design, and optimize tissue engineering scaffolds, with a potential in 3D printing fabrication, J. Biomed. Mater. Res. B Appl. Biomater. 107 (5) (2019) 1329–1351.
[74] H. Cui, et al., 3D bioprinting for organ regeneration, Adv. Healthc. Mater. 6 (1) (2017) 1601118.
[75] M. Yeo, G. Kim, Micro/nano-hierarchical scaffold fabricated using a cell electrospinning/3D printing process for co-culturing myoblasts and HUVECs to induce myoblast alignment and differentiation, Acta Biomater. 107 (2020) 102–114.
[76] A. Behre, et al., 3D bioprinted patient-specific extracellular matrix scaffolds for soft tissue defects, Adv. Healthc. Mater. 11 (24) (2022) 2200866.
[77] E.H.Y. Lam, et al., 3D bioprinting for next-generation personalized medicine, Int. J. Mol. Sci. 24 (7) (2023) 6357.
[78] K. Osouli-Bostanabad, et al., Traction of 3D and 4D printing in the healthcare industry: From drug delivery and analysis to regenerative medicine, ACS Biomater. Sci. Eng. 8 (7) (2022) 2764–2797.
[79] Y. Zhang, et al., Recent advances in 3D bioprinting of vascularized tissues, Mater. Des. 199 (2021) 109398.
[80] M. Yeo, et al., Synergistic coupling between 3D bioprinting and vascularization strategies, Biofabrication 16 (1) (2023) 012003.
[81] A. Mir, et al., 3D Bioprinting for Vascularization, Bioengineering 10 (5) (2023) 606.
[82] V. Lee, et al., Design and fabrication of human skin by three-dimensional bioprinting, Tissue Eng. Part C Methods 20 (6) (2014) 473–484.
[83] Y. Gilaberte, et al., Anatomy and Function of the Skin, in: Nanoscience in Dermatology, Elsevier, 2016, pp. 1–14.
[84] F. Bonté, et al., Skin changes during ageing, Part II Clinical Science, Biochemistry and Cell Biology of Ageing, 2019, pp. 249–280.
[85] N. Cubo, et al., 3D bioprinting of functional human skin: production and in vivo analysis, Biofabrication 9 (1) (2016) 015006.
[86] A.G. Haddad, et al., Skin substitutes and bioscaffolds: temporary and permanent coverage, Clin. Plast. Surg. 44 (3) (2017) 627–634.
[87] W.L. Ng, W.Y. Yeong, The future of skin toxicology testing–Three-dimensional bioprinting meets microfluidics, Int. J. Bioprinting 5 (2.1) (2019).
[88] L. Pontiggia, et al., Bioprinting and plastic compression of large pigmented and vascularized human dermo-epidermal skin substitutes by means of a new robotic platform, J. Tissue Eng. 13 (2022), 20417314221088513.
[89] Y. Wang, et al., Application of bioprinting in ophthalmology, Int. J. Bioprinting 8 (2) (2022).
[90] Z. Li, et al., Silk fibroin–gelatin photo-crosslinked 3D-bioprinted hydrogel with MOF-methylene blue nanoparticles for infected wound healing, Int. J. Bioprinting 9 (5) (2023).
[91] H. Fu, et al., Application of 3D-printed tissue-engineered skin substitute using innovative biomaterial loaded with human adipose-derived stem cells in wound healing, Int. J. Bioprinting 9 (2) (2023).
[92] Y. Yang, et al., Recombinant human collagen-based bioinks for the 3D bioprinting of full-thickness human skin equivalent, Int. J. Bioprinting 8 (4) (2022).
[93] J. Wu, et al., 3D bioprinting of calcium molybdate nanoparticles-containing immunomodulatory bioinks for hair regrowth, Nano Today 51 (2023) 101917.
[94] D. Kang, et al., 3D bioprinting of a gelatin-alginate hydrogel for tissue-engineered hair follicle regeneration, Acta Biomater. 165 (2023) 19–30.
[95] W. Zhao, et al., Adaptive multi-degree-of-freedom in situ bioprinting robot for hair-follicle-inclusive skin repair: A preliminary study conducted in mice, Bioeng. Transl. Med. 7 (3) (2022) e10303.
[96] Z. Abbas, et al., Toughening of Bioceramic Composites for Bone Regeneration, Journal of Composites Science 5 (10) (2021) 259.
[97] J. Li, et al., 3D printing of hydrogels: Rational design strategies and emerging biomedical applications, Mater. Sci. Eng. R. Rep. 140 (2020) 100543.
[98] Jariwala, S.H., et al., *3D printing of personalized artificial bone scaffolds.* 3D printing and additive manufacturing, 2015. 2(2): p. 56-64.
[99] A. Pacifici, et al., Decellularized hydrogels in bone tissue engineering: a topical review, Int. J. Med. Sci. 15 (5) (2018) 492.
[100] L. Zhang, et al., Three-dimensional (3D) printed scaffold and material selection for bone repair, Acta Biomater. 84 (2019) 16–33.
[101] Y. Huan, et al., 3D bioprinted autologous bone particle scaffolds for cranioplasty promote bone regeneration with both implanted and native BMSCs, Biofabrication 15 (2) (2023) 025016.
[102] M. Shen, et al., 3D bioprinting of in situ vascularized tissue engineered bone for repairing large segmental bone defects, Mater. Today Biol. 16 (2022) 100382.
[103] Z. Li, et al., 3D bioprinted gelatin/gellan gum-based scaffold with double-crosslinking network for vascularized bone regeneration, Carbohydr. Polym. 290 (2022) 119469.
[104] J. Tao, et al., DLP-based bioprinting of void-forming hydrogels for enhanced stem-cell-mediated bone regeneration, Mater. Today Biol. 17 (2022) 100487.
[105] H. Tang, et al., 3D-bioprinted recombination structure of Hertwig's epithelial root sheath cells and dental papilla cells for alveolar bone regeneration, Int. J. Bioprinting 8 (3) (2022).
[106] W. Schuurman, et al., Cartilage regeneration using zonal chondrocyte subpopulations: a promising approach or an overcomplicated strategy? J. Tissue Eng. Regen. Med. 9 (6) (2015) 669–678.
[107] W. Wei, H. Dai, Articular cartilage and osteochondral tissue engineering techniques: Recent advances and challenges, Bioact. Mater. 6 (12) (2021) 4830–4855.
[108] Mota, C., et al., *Bioprinting: From Tissue and Organ Development to*. 2020, Vitro.
[109] E.E. Beketov, et al., Bioprinting of Cartilage with Bioink Based on High-Concentration Collagen and Chondrocytes, Int. J. Mol. Sci. 22 (21) (2021) 11351.
[110] J. Huang, et al., 3D bioprinting of hydrogels for cartilage tissue engineering, Gels 7 (3) (2021) 144.
[111] Y. Han, et al., Study on bioactive PEGDA/ECM hybrid bi-layered hydrogel scaffolds fabricated by electro-writing for cartilage regeneration, Appl. Mater. Today 28 (2022) 101547.

[112] Q. Wei, et al., Design and evaluation of sodium alginate/polyvinyl alcohol blend hydrogel for 3D bioprinting cartilage scaffold: molecular dynamics simulation and experimental method, J. Mater. Res. Technol. 17 (2022) 66–78.
[113] J. Chakraborty, et al., Development of a biomimetic arch-like 3D bioprinted construct for cartilage regeneration using gelatin methacryloyl and silk fibroin-gelatin bioinks, Biofabrication 15 (3) (2023) 035009.
[114] Z. Pei, et al., Experimental study on repair of cartilage defects in the rabbits with GelMA-MSCs scaffold prepared by three-dimensional bioprinting, Int. J. Bioprinting 9 (2) (2023).
[115] L. Jia, et al., Bioprinting and regeneration of auricular cartilage using a bioactive bioink based on microporous photocrosslinkable acellular cartilage matrix, Bioact. Mater. 16 (2022) 66–81.
[116] J. Zeng, et al., Bacterial nanocellulose-reinforced gelatin methacryloyl hydrogel enhances biomechanical property and glycosaminoglycan content of 3D-bio-printed cartilage, Int. J. Bioprinting 9 (1) (2023).
[117] M. Thangadurai, et al., *Advances in electrospinning and 3D bioprinting strategies to enhance functional regeneration of skeletal muscle tissue.* Biomater. Adv. (2022) 213135.
[118] S. Ostrovidov, et al., 3D bioprinting in skeletal muscle tissue engineering, Small 15 (24) (2019) 1805530.
[119] P. Zhuang, et al., Bioprinting of 3D in vitro skeletal muscle models: A review, Mater. Des. 193 (2020) 108794.
[120] T. Li, et al., Bioprinted anisotropic scaffolds with fast stress relaxation bioink for engineering 3D skeletal muscle and repairing volumetric muscle loss, Acta Biomater. 156 (2023) 21–36.
[121] E. Fornetti, et al., A novel extrusion-based 3D bioprinting system for skeletal muscle tissue engineering, Biofabrication 15 (2) (2023) 025009.
[122] T. Fan, et al., Controllable assembly of skeletal muscle-like bundles through 3D bioprinting, Biofabrication 14 (1) (2021) 015009.
[123] F.L. Ronzoni, et al., Myoblast 3D bioprinting to burst in vitro skeletal muscle differentiation, J. Tissue Eng. Regen. Med. 16 (5) (2022) 484–495.
[124] W. Su, et al., Gradient composite film with calcium phosphate silicate for improved tendon-to-Bone intergration, Chem. Eng. J. 404 (2021) 126473.
[125] S. Chae, D.-W. Cho, Biomaterial-based 3D bioprinting strategy for orthopedic tissue engineering, Acta Biomater. 156 (2023) 4–20.
[126] C. Ning, et al., Recent advances in tendon tissue engineering strategy, Front. Bioeng. Biotechnol. 11 (2023) 1115312.
[127] F. Al-Hakim Khalak, et al., Decellularized extracellular matrix-based bioinks for tendon regeneration in three-dimensional bioprinting, Int. J. Mol. Sci. 23 (21) (2022) 12930.
[128] R. Gottardi, et al., Application of a hyperelastic 3D printed scaffold for mesenchymal stem cell-based fabrication of a bizonal tendon enthesis-like construct, Front. Mater. 8 (2021) 613212.
[129] X. Jiang, et al., 3D printing of multilayered scaffolds for rotator cuff tendon regeneration, Bioact. Mater. 5 (3) (2020) 636–643.
[130] S. Laternser, et al., A novel microplate 3D bioprinting platform for the engineering of muscle and tendon tissues, SLAS Technology: Translating Life Sciences Innovation 23 (6) (2018) 599–613.
[131] C. Li, et al., 3D-printed hydrogel particles containing PRP laden with TDSCs promote tendon repair in a rat model of tendinopathy, J. Nanobiotechnol. 21 (1) (2023) 177.
[132] L. Du, et al., Multicellular bioprinting of biomimetic inks for tendon-to-bone regeneration, Adv. Sci. (2023) 2301309.
[133] A. Farzin, et al., *Scaffolds in dental tissue engineering: A review.* Arch. Neurosci. 7 (1) (2020).
[134] S. Raees, et al., Classification, processing, and applications of bioink and 3D bioprinting: A detailed review, Int. J. Biol. Macromol. (2023) 123476.
[135] S. Ostrovidov, et al., Bioprinting and biomaterials for dental alveolar tissue regeneration, Front. Bioeng. Biotechnol. 11 (2023) 991821.
[136] D. Nesic, et al., 3D printing approach in dentistry: the future for personalized oral soft tissue regeneration, J. Clin. Med. 9 (7) (2020) 2238.
[137] U.-L. Lee, et al., Bioprinting on 3D printed titanium scaffolds for periodontal ligament regeneration, Cells 10 (6) (2021) 1337.
[138] J.H. Park, et al., The effect of BMP-mimetic peptide tethering bioinks on the differentiation of dental pulp stem cells (DPSCs) in 3D bioprinted dental constructs, Biofabrication 12 (3) (2020) 035029.
[139] J. Han, et al., Demineralized dentin matrix particle-based bio-ink for patient-specific shaped 3D dental tissue regeneration, Polymers 13 (8) (2021) 1294.
[140] P. Shi, et al., A bilayer photoreceptor-retinal tissue model with gradient cell density design: a study of microvalve-based bioprinting, J. Tissue Eng. Regen. Med. 12 (5) (2018) 1297–1306.
[141] S. Li, et al., Applications of hydrogel materials in different types of corneal wounds, Surv. Ophthalmol. (2023).
[142] S. Jia, et al., Advances in 3D bioprinting technology for functional corneal reconstruction and regeneration, Front. Bioeng. Biotechnol. 10 (2023) 1065460.
[143] Y. Xu, et al., *Biomimetic convex implant for corneal regeneration through 3D printing*, Adv. Sci. (2023) 2205878.
[144] H. Kim, et al., Shear-induced alignment of collagen fibrils using 3D cell printing for corneal stroma tissue engineering, Biofabrication 11 (3) (2019) 035017.
[145] D.F. Duarte Campos, et al., Corneal bioprinting utilizing collagen-based bioinks and primary human keratocytes, J. Biomed. Mater. Res. Part A 107 (9) (2019) 1945–1953.
[146] B. He, et al., 3D printed biomimetic epithelium/stroma bilayer hydrogel implant for corneal regeneration, Bioact. Mater. 17 (2022) 234–247.
[147] S. Fleischer, D.N. Tavakol, G. Vunjak-Novakovic, From arteries to capillaries: approaches to engineering human vasculature, Adv. Funct. Mater. 30 (37) (2020) 1910811.
[148] R. Othman, et al., An automated fabrication strategy to create patterned tubular architectures at cell and tissue scales, Biofabrication 7 (2) (2015) 025003.
[149] E.C. Novosel, C. Kleinhans, P.J. Kluger, Vascularization is the key challenge in tissue engineering, Adv. Drug Deliv. Rev. 63 (4–5) (2011) 300–311.
[150] J. Jang, 3D bioprinting and in vitro cardiovascular tissue modeling, Bioengineering 4 (3) (2017) 71.
[151] B. Duan, State-of-the-art review of 3D bioprinting for cardiovascular tissue engineering, Ann. Biomed. Eng. 45 (1) (2017) 195–209.
[152] Z. Zhang, et al., A multi-axis robot-based bioprinting system supporting natural cell function preservation and cardiac tissue fabrication, Bioact. Mater. 18 (2022) 138–150.
[153] Q. Jin, et al., Nanofiber electrospinning combined with rotary bioprinting for fabricating small-diameter vessels with endothelium and smooth muscle, Compos. B Eng. 234 (2022) 109691.
[154] M.E. Jewett, et al., Rapid magnetically directed assembly of pre-patterned capillary-scale microvessels, Adv. Funct. Mater. (2023) 2203715.
[155] X. Zhou, et al., 3D-bioprinted vascular scaffold with tunable mechanical properties for simulating and promoting neo-vascularization, Smart Materials in Medicine 3 (2022) 199–208.
[156] N. Liu, et al., Advances in 3D bioprinting technology for cardiac tissue engineering and regeneration, Bioact. Mater. 6 (5) (2021) 1388–1401.
[157] Y. Jiang, X.L. Lian, Heart regeneration with human pluripotent stem cells: prospects and challenges, Bioact. Mater. 5 (1) (2020) 74–81.
[158] F.K. Kozaniti, et al., Recent advancements in 3D printing and bioprinting methods for cardiovascular tissue engineering, Bioengineering 8 (10) (2021) 133.
[159] C.D. Roche, et al., Current challenges in three-dimensional bioprinting heart tissues for cardiac surgery, Eur. J. Cardiothorac. Surg. 58 (3) (2020) 500–510.
[160] A.D. Cetnar, et al., Patient-specific 3D bioprinted models of developing human heart, Adv. Healthc. Mater. 10 (15) (2021) 2001169.
[161] C.D. Roche, et al., Printability, durability, contractility and vascular network formation in 3D bioprinted cardiac endothelial cells using alginate–gelatin hydrogels, Front. Bioeng. Biotechnol. 9 (2021) 636257.
[162] L. Polonchuk, et al., Towards engineering heart tissues from bioprinted cardiac spheroids, Biofabrication 13 (4) (2021) 045009.
[163] P. Zhuang, et al., 3D neural tissue models: From spheroids to bioprinting, Biomaterials 154 (2018) 113–133.
[164] E. Moeendarbary, et al., The soft mechanical signature of glial scars in the central nervous system, Nat. Commun. 8 (1) (2017) 1–11.
[165] C.E. Schmidt, J.B. Leach, Neural tissue engineering: strategies for repair and regeneration, Annu. Rev. Biomed. Eng. 5 (1) (2003) 293–347.
[166] C.M. Owens, et al., Biofabrication and testing of a fully cellular nerve graft, Biofabrication 5 (4) (2013) 045007.
[167] S. Knowlton, et al., Bioprinting for neural tissue engineering, Trends Neurosci. 41 (1) (2018) 31–46.
[168] M. Restan Perez, et al., 3D Bioprinting mesenchymal stem cell-derived neural tissues using a fibrin-based bioink, Biomolecules 11 (8) (2021) 1250.
[169] S. Song, et al., Neural stem cell-laden 3D bioprinting of polyphenol-doped electroconductive hydrogel scaffolds for enhanced neuronal differentiation, Mater. Sci. Eng. C (2022) 112639.
[170] J. Yang, et al., 3D bio-printed living nerve-like fibers refine the ecological niche for long-distance spinal cord injury regeneration, Bioact. Mater. 25 (2023) 160–175.
[171] Wang, S., et al., 3D bioprinting of neurovascular tissue modeling with collagen-based low-viscosity composites. Adv. Healthcare Mater.: p. 2300004.
[172] G.K. Michalopoulos, Liver regeneration, J. Cell. Physiol. 213 (2) (2007) 286–300.
[173] K.D. Pluta, et al., Cell-based clinical and experimental methods for assisting the function of impaired livers–Present and future of liver support systems, Biocybernet. Biomed. Eng. 41 (4) (2021) 1322–1346.
[174] T. Itoh, Stem/progenitor cells in liver regeneration, Hepatology 64 (2) (2016) 663–668.
[175] I. Matai, et al., Progress in 3D bioprinting technology for tissue/organ regenerative engineering, Biomaterials 226 (2020) 119536.
[176] H. Jian, et al., In vitro construction of liver organoids with biomimetic lobule structure by a multicellular 3D bioprinting strategy, Cell Prolif. (2023) e13465.
[177] L. Jaksa, et al., 3D-Printed multi-material liver model with simultaneous mechanical and radiological tissue-mimicking features for improved realism, Int. J. Bioprinting 9 (4) (2023).
[178] J. Wang, et al., Biomimic trained immunity-MSCs delivery microcarriers for acute liver failure regeneration, Small (2022) 2200858.
[179] Q. Mao, et al., Fabrication of liver microtissue with liver decellularized extracellular matrix (dECM) bioink by digital light processing (DLP) bioprinting, Mater. Sci. Eng. C 109 (2020) 110625.
[180] A.M. Chibly, et al., Salivary gland function, development, and regeneration, Physiol. Rev. 102 (3) (2022) 1495–1552.
[181] S. Khan, et al., Exocrine gland structure-function relationships, Development 149 (1) (2022) dev197657.
[182] R. Lauretta, et al., Endocrine disrupting chemicals: effects on endocrine glands, Front. Endocrinol. 10 (2019) 178.
[183] X. Yuan, et al., Reciprocal interaction between vascular niche and sweat gland promotes sweat gland regeneration, Bioact. Mater. 21 (2023) 340–357.
[184] C. Adine, et al., Engineering innervated secretory epithelial organoids by magnetic three-dimensional bioprinting for stimulating epithelial growth in salivary glands, Biomaterials 180 (2018) 52–66.

[185] T. Rodboon, et al., Magnetic bioassembly platforms for establishing craniofacial exocrine gland organoids as aging in vitro models, PLoS One 17 (8) (2022) e0272644.
[186] Y. Xu, D. Song, X. Wang, 3D bioprinting for pancreas engineering/manufacturing, Polymers 14 (23) (2022) 5143.
[187] H. Peng, et al., SnRNA-Seq of pancreas revealed the dysfunction of endocrine and exocrine cells in transgenic pigs with prediabetes, Int. J. Mol. Sci. 24 (9) (2023) 7701.
[188] K.J. Stevens, and C, Lisanti, Pancreas imaging, 2019.
[189] L. Jiang, et al., Making human pancreatic islet organoids: Progresses on the cell origins, biomaterials and three-dimensional technologies, Theranostics 12 (4) (2022) 1537.
[190] X. Liu, et al., Development of a coaxial 3D printing platform for biofabrication of implantable islet-containing constructs, Adv. Healthc. Mater. 8 (7) (2019) 1801181.
[191] G.A. Salg, et al., Toward 3D-bioprinting of an endocrine pancreas: A building-block concept for bioartificial insulin-secreting tissue, J. Tissue Eng. 13 (2022), 20417314221091033.
[192] D. Wang, et al., Hyaluronic acid methacrylate/pancreatic extracellular matrix as a potential 3D printing bioink for constructing islet organoids, Acta Biomater. (2022).
[193] E.A. Al-Suhaimi, F.A. Khan, Thyroid Glands: Physiology and Structure, in: Emerging Concepts in Endocrine Structure and Functions, Springer, 2022, pp. 133–160.
[194] E.A. Bulanova, et al., Bioprinting of a functional vascularized mouse thyroid gland construct, Biofabrication 9 (3) (2017) 034105.
[195] M. Barreiro Carpio, et al., 3D Bioprinting strategies, challenges, and opportunities to model the lung tissue microenvironment and its function, Front. Bioeng. Biotechnol. 9 (2021) 773511.
[196] Mahfouzi, S., S. Tali, and G. Amoabediny, 3D bioprinting for lung and tracheal tissue engineering: criteria, advances, challenges, and future directions. Bioprinting. 2021; 21: e00124. Elsevier. doi.
[197] W.L. Ng, et al., Fabrication and characterization of 3D bioprinted triple-layered human alveolar lung models, Int. J. Bioprinting 7 (2) (2021).
[198] F.S. Rezaei, et al., 3D printed chitosan/polycaprolactone scaffold for lung tissue engineering: hope to be useful for COVID-19 studies, RSC Adv. 11 (32) (2021) 19508–19520.
[199] J. Berg, et al., Optimization of cell-laden bioinks for 3D bioprinting and efficient infection with influenza A virus, Sci. Rep. 8 (1) (2018) 13877.
[200] N.N. da Rosa, et al., Three-Dimensional Bioprinting of an In Vitro Lung Model, Int. J. Mol. Sci. 24 (6) (2023) 5852.
[201] O. Jung, et al., Development of human-derived, three-dimensional respiratory epithelial tissue constructs with perfusable microvasculature on a high-throughput microfluidics screening platform, Biofabrication 14 (2) (2022) 025012.
[202] K. Xu, et al., The application of 3D bioprinting in urological diseases, Mater. Today Biol. (2022) 100388.
[203] Y. Zhao, et al., Application of 3D Bioprinting in Urology, Micromachines 13 (7) (2022) 1073.
[204] Z. Wang, et al., Tissue-specific engineering: 3D bioprinting in regenerative medicine, J. Controll. Release 329 (2021) 237–256.
[205] N.M. Wragg, L. Burke, S.L. Wilson, A critical review of current progress in 3D kidney biomanufacturing: Advances, challenges, and recommendations, Renal Replacement Therapy 5 (1) (2019) 1–16.
[206] B.D. Humphreys, Bioprinting better kidney organoids, Nat. Mater. 20 (2) (2021) 128–130.
[207] M. Ali, et al., A photo-crosslinkable kidney ECM-derived bioink accelerates renal tissue formation, Adv. Healthc. Mater. 8 (7) (2019) 1800992.
[208] K. Tröndle, et al., Scalable fabrication of renal spheroids and nephron-like tubules by bioprinting and controlled self-assembly of epithelial cells, Biofabrication 13 (3) (2021) 035019.
[209] Z. Chen, L.-T. Zhu, Z.-H. Luo, Characterizing flow and transport in biological vascular systems: a review from physiological and chemical engineering perspectives, Ind. Eng. Chem. Res. (2023).
[210] Y. Ibi, R. Nishinakamura, Kidney Bioengineering for Transplantation, Transplantation (2023), 0000000000004526.
[211] K.T. Lawlor, et al., Cellular extrusion bioprinting improves kidney organoid reproducibility and conformation, Nat. Mater. 20 (2) (2021) 260–271.
[212] K. Zhang, et al., 3D bioprinting of urethra with PCL/PLCL blend and dual autologous cells in fibrin hydrogel: An in vitro evaluation of biomimetic mechanical property and cell growth environment, Acta Biomater. 50 (2017) 154–164.
[213] S. Chae, et al., 3D Bioprinting of an in vitro model of a biomimetic urinary bladder with a contract-release system, Micromachines 13 (2) (2022) 277.
[214] L. Alzamil, K. Nikolakopoulou, M.Y. Turco, Organoid systems to study the human female reproductive tract and pregnancy, Cell Death Differ. 28 (1) (2021) 35–51.
[215] Y. Cui, et al., Human female reproductive system organoids: applications in developmental biology, disease modelling, and drug discovery, Stem Cell Rev. Rep. 16 (2020) 1173–1184.
[216] S. Antonouli, et al., A comprehensive review and update on human fertility cryopreservation methods and tools, Front. Veterinary Sci. 10 (2023) 1151254.
[217] A. Kirillova, et al., Bioethical and legal issues in 3D bioprinting, Int. J. Bioprinting 6 (3) (2020).
[218] Y. Zhu, et al., Developing biomedical engineering technologies for reproductive medicine, Smart Med. 1 (1) (2022) e20220006.
[219] M.M. Laronda, et al., Initiation of puberty in mice following decellularized ovary transplant, Biomaterials 50 (2015) 20–29.
[220] J. Zheng, et al., Ovary-derived decellularized extracellular matrix-based bioink for fabricating 3D primary ovarian cells-laden structures for mouse ovarian failure correction, Int. J. Bioprinting 8 (3) (2022).
[221] T. Wu, et al., Three-dimensional bioprinting of artificial ovaries by an extrusion-based method using gelatin-methacryloyl bioink, Climacteric 25 (2) (2022) 170–178.
[222] W. Ji, et al., 3D Bioprinting a human iPSC-derived MSC-loaded scaffold for repair of the uterine endometrium, Acta Biomater. 116 (2020) 268–284.
[223] E. Frances-Herrero, et al., Bioengineering trends in female reproduction: a systematic review, Hum. Reprod. Update 28 (6) (2022) 798–837.
[224] G.R. Souza, et al., Magnetically bioprinted human myometrial 3D cell rings as a model for uterine contractility, Int. J. Mol. Sci. 18 (4) (2017) 683.
[225] N. Nie, et al., 3D bio-printed endometrial construct restores the full-thickness morphology and fertility of injured uterine endometrium, Acta Biomater. 157 (2023) 187–199.
[226] W. Zhao, et al., Subaqueous bioprinting: a novel strategy for fetal membrane repair with 7-axis robot-assisted minimally invasive surgery, Adv. Funct. Mater. 32 (51) (2022) 2207496.
[227] M. Robinson, et al., Using clinically derived human tissue to 3-dimensionally bioprint personalized testicular tubules for in vitro culturing: first report, F&S Science 3 (2) (2022) 130–139.
[228] Z. Bashiri, et al., In vitro production of mouse morphological sperm in artificial testis bioengineered by 3D printing of extracellular matrix, Int. J. Biol. Macromol. 217 (2022) 824–841.
[229] Q. Lihao, et al., 3D bioprinting of Salvianolic acid B-sodium alginate-gelatin skin scaffolds promotes diabetic wound repair via antioxidant, anti-inflammatory, and proangiogenic effects, Biomed. Pharmacother. 171 (2024) 116168.
[230] D. Zhang, et al., 3D-bioprinted human lipoaspirate-derived cell-laden skin constructs for healing of full-thickness skin defects, Int. J. Bioprinting 9 (4) (2023).
[231] K. Khoshmaram, et al., Preparation and characterization of 3D bioprinted gelatin methacrylate hydrogel incorporated with curcumin loaded chitosan nanoparticles for in vivo wound healing application, Biomater. Adv. 156 (2024) 213677.
[232] M. Li, et al., 3D bioprinting of heterogeneous tissue-engineered skin containing human dermal fibroblasts and keratinocytes, Biomater. Sci. 11 (7) (2023) 2461–2477.
[233] S. Afra, et al., Chitosan/Nanohydroxyapatite/Hydroxyethyl-cellulose-based printable formulations for local alendronate drug delivery in osteoporosis treatment, Carbohydr. Polym. Technol. Appl. 7 (2024) 100418.
[234] Y.-F. Wu, et al., 3D-bioprinted alginate-based bioink scaffolds with β-tricalcium phosphate for bone regeneration applications, J. Dental Sci. (2024).
[235] Y. Zhang, et al., *3D-bioprinted anisotropic bicellular living hydrogels boost osteochondral regeneration via reconstruction of cartilage–bone interface*, Innovation 5 (1) (2024).
[236] H. Shi, et al., Advantages of photo-curable collagen-based cell-laden bioinks compared to methacrylated gelatin (GelMA) in digital light processing (DLP) and extrusion bioprinting, Mater. Today Biol. 23 (2023) 100799.
[237] X.R. Li, et al., Three-dimensional printed biomimetic multilayer scaffolds coordinated with sleep-related small extracellular vesicles: A strategy for extracellular matrix homeostasis and macrophage polarization to enhance osteochondral regeneration, View (2024) 20230069.
[238] D.G. O'Shea, et al., An injectable and 3D printable pro-chondrogenic hyaluronic acid and collagen type II composite hydrogel for the repair of articular cartilage defects, Biofabrication 16 (1) (2023) 015007.
[239] T.H. Jovic, et al., A comparative analysis of pulp-derived nanocelluloses for 3D bioprinting facial cartilages, Carbohydr. Polym. 321 (2023) 121261.
[240] S. Jahangir, et al., Cell-Laden 3D printed GelMA/HAp and THA hydrogel bioinks: development of osteochondral tissue-like bioinks, Materials 16 (22) (2023) 7214.
[241] J. Lee, et al., 3D bioprinting using a new photo-crosslinking method for muscle tissue restoration, npj Regener. Med. 8 (1) (2023) 18.
[242] S. Boularaoui, et al., Nanocomposite conductive bioinks based on low-concentration GelMA and MXene nanosheets/gold nanoparticles providing enhanced printability of functional skeletal muscle tissues, ACS Biomater. Sci. Eng. 7 (12) (2021) 5810–5822.
[243] P. Puistola, et al., Novel strategy for multi-material 3D bioprinting of human stem cell based corneal stroma with heterogenous design, Mater. Today Biol. 24 (2024) 100924.
[244] M. Zhang, et al., 3D bioprinting of corneal decellularized extracellular matrix: GelMA composite hydrogel for corneal stroma engineering, Int. J. Bioprinting 9 (5) (2023).
[245] S.S. Mahdavi, et al., Stereolithography 3D bioprinting method for fabrication of human corneal stroma equivalent, Ann. Biomed. Eng. 48 (2020) 1955–1970.
[246] F. Lackner, et al., 4-axis 3D-printed tubular biomaterials imitating the anisotropic nanofiber orientation of porcine aortae, Adv. Healthc. Mater. (2023) 2302348.
[247] C.D. Roche, et al., 3D bioprinted alginate-gelatin hydrogel patches containing cardiac spheroids recover heart function in a mouse model of myocardial infarction, Bioprinting 30 (2023) e00263.
[248] S. Lee, et al., Human-recombinant-Elastin-based bioinks for 3D bioprinting of vascularized soft tissues, Adv. Mater. 32 (45) (2020) 2003915.
[249] Y.J. Shin, et al., 3D bioprinting of mechanically tuned bioinks derived from cardiac decellularized extracellular matrix, Acta Biomater. 119 (2021) 75–88.
[250] E.M. Cruz, et al., A gelatin methacrylate-based hydrogel as a potential bioink for 3D bioprinting and neuronal differentiation, Pharmaceutics 15 (2) (2023) 627.

[251] M.A. Sullivan, et al., Three-dimensional bioprinting of stem cell-derived central nervous system cells enables astrocyte growth, vasculogenesis, and enhances neural differentiation/function, Biotechnol. Bioeng. 120 (10) (2023) 3079–3091.
[252] Y. Li, et al., Coaxial 3D printing of hierarchical structured hydrogel scaffolds for on-demand repair of spinal cord injury, Acta Biomater. 168 (2023) 400–415.
[253] L. De la Vega, et al., 3D bioprinting human-induced pluripotent stem cells and drug-releasing microspheres to produce responsive neural tissues, Adv. NanoBiomed Res. 1 (8) (2021) 2000077.
[254] Y. Wu, et al., 3D bioprinting of bicellular liver lobule-mimetic structures via microextrusion of cellulose nanocrystal-incorporated shear-thinning bioink, Sci. Rep. 10 (1) (2020) 20648.
[255] V. Khati, et al., 3D bioprinting of multi-material decellularized liver matrix hydrogel at physiological temperatures, Biosensors 12 (7) (2022) 521.
[256] V. Khati, et al., Indirect 3d bioprinting of a robust trilobular hepatic construct with decellularized liver matrix hydrogel, Bioengineering 9 (11) (2022) 603.
[257] Y. Zhang, et al., Using bioprinting and spheroid culture to create a skin model with sweat glands and hair follicles, Burns Trauma 9 (2021) tkab013.
[258] B. Yao, et al., Biochemical and structural cues of 3D-printed matrix synergistically direct MSC differentiation for functional sweat gland regeneration, Sci. Adv. 6 (10) (2020) eaaz1094.
[259] Y. Wang, et al., Notch4 participates in mesenchymal stem cell-induced differentiation in 3D-printed matrix and is implicated in eccrine sweat gland morphogenesis, Burns Trauma 11 (2023) tkad032.
[260] I.T. Ozbolat, Bioprinting scale-up tissue and organ constructs for transplantation, Trends Biotechnol. 33 (7) (2015) 395–400.
[261] A. Arslan-Yildiz, et al., Towards artificial tissue models: past, present, and future of 3D bioprinting, Biofabrication 8 (1) (2016) 014103.
[262] Z. Gu, et al., Development of 3D bioprinting: From printing methods to biomedical applications, Asian J. Pharm. Sci. 15 (5) (2020) 529–557.
[263] H.-W. Kang, et al., A 3D bioprinting system to produce human-scale tissue constructs with structural integrity, Nat. Biotechnol. 34 (3) (2016) 312–319.
[264] D.M. Kirchmajer, R. Gorkin Iii, An overview of the suitability of hydrogel-forming polymers for extrusion-based 3D-printing, J. Mater. Chem. B 3 (20) (2015) 4105–4117.
[265] A. Panwar, L.P. Tan, Current status of bioinks for micro-extrusion-based 3D bioprinting, Molecules 21 (6) (2016) 685.
[266] K.A. Deo, et al., Bioprinting 101: design, fabrication, and evaluation of cell-laden 3D bioprinted scaffolds, Tissue Eng. A 26 (5–6) (2020) 318–338.
[267] S.V. Murphy, P. De Coppi, A. Atala, Opportunities and challenges of translational 3D bioprinting, Nat. Biomed. Eng. 4 (4) (2020) 370–380.
[268] H. Xu, et al., Investigation of Cell Aggregation on the Printing Performance in Inkjet-Based Bioprinting of Cell-Laden Bioink, Langmuir 39 (1) (2022) 545–555.
[269] H.-Q. Xu, et al., A review on cell damage, viability, and functionality during 3D bioprinting, Mil. Med. Res. 9 (1) (2022) 70.
[270] W.L. Ng, et al., Controlling droplet impact velocity and droplet volume: Key factors to achieving high cell viability in sub-nanoliter droplet-based bioprinting, Int. J. Bioprinting 8 (1) (2022).
[271] S.J. Hollister, Porous scaffold design for tissue engineering, Nat. Mater. 4 (7) (2005) 518–524.
[272] I.T. Ozbolat, W. Peng, V. Ozbolat, Application areas of 3D bioprinting, Drug Discov. Today 21 (8) (2016) 1257–1271.
[273] F. Gilbert, et al., Print me an organ? Ethical and regulatory issues emerging from 3D bioprinting in medicine, Sci. Eng. Ethics 24 (1) (2018) 73–91.
[274] F. Mota, et al., 3D and 4D bioprinted human model patenting and the future of drug development, Nature Publishing Group, 2020.
[275] X. Cui, et al., Advances in extrusion 3D bioprinting: a focus on multicomponent hydrogel-based bioinks, Adv. Healthc. Mater. 9 (15) (2020) 1901648.
[276] A. Nadernezhad, et al., Multifunctional 3D printing of heterogeneous hydrogel structures, Sci. Rep. 6 (1) (2016) 1–12.
[277] A.L. Rutz, et al., A multimaterial bioink method for 3D printing tunable, cell-compatible hydrogels, Adv. Mater. 27 (9) (2015) 1607–1614.